Flow Research Report No. 482

DEVELOPMENT OF A SCANNING LASER VELOCIMETER FOR COASTAL AND MARINE APPLICATIONS

- Phase I Feasibility Investigation -

H.-T. Liu

August 1989

Prepared for the
OFFICE OF NAVAL RESEARCH
Under Contract No. N00014-88-C-0682
Contract Period: 1 October 1988 - 31 May 1989

Flow Research, Inc.
21414 - 68th Avenue South
Kent, Washington 98032
(206) 872-8500

REPORT DOCUMENTATION PAGE

Form Approved OMB No 0704-0188

1a. REPORT SECURITY CLASSIFICATION Unclassified	1b. RESTRICTIVE MARKINGS
2a. SECURITY CLASSIFICATION AUTHORITY	3. DISTRIBUTION/AVAILABILITY OF REPORT Distribution Unlimited; Approved for Public Release
2b. DECLASSIFICATION/DOWNGRADING SCHEDULE	
4. PERFORMING ORGANIZATION REPORT NUMBER(S) Flow Research Report No. 482	5. MONITORING ORGANIZATION REPORT NUMBER(S)
6a. NAME OF PERFORMING ORGANIZATION Flow Research, Inc. 6b. OFFICE SYMBOL (If applicable)	7a. NAME OF MONITORING ORGANIZATION DCASMA Seattle
6c. ADDRESS (City, State, and ZIP Code) 21414 - 68th Avenue South Kent, WA 98032	7b. ADDRESS (City, State, and ZIP Code) Bldg. SD Naval Station Seattle, WA 98115-5010
8a. NAME OF FUNDING/SPONSORING ORGANIZATION Office of Naval Research 8b. OFFICE SYMBOL (If applicable) N00014	9 PROCUREMENT INSTRUMENT IDENTIFICATION NUMBER N00014-88-C-0682
8c. ADDRESS (City, State, and ZIP Code) Department of the Navy 800 N. Quincy Street Arlington, VA 22217	10. SOURCE OF FUNDING NUMBERS PROGRAM ELEMENT NO. / PROJECT NO. / TASK NO / WORK UNIT ACCESSION NO.

11. TITLE (Include Security Classification)
DEVELOPMENT OF A SCANNING LASER VELOCIMETER FOR COASTAL AND MARINE APPLICATIONS: Phase I Feasibility Investigation

12. PERSONAL AUTHOR(S)
H.-T. Liu

13a. TYPE OF REPORT	13b. TIME COVERED	14. DATE OF REPORT (Year, Month, Day)	15. PAGE COUNT
Final	FROM 10-88 TO 5-89	August 1989	42

16. SUPPLEMENTARY NOTATION

17. COSATI CODES			18. SUBJECT TERMS (Continue on reverse if necessary and identify by block number)
FIELD	GROUP	SUB-GROUP	laser diodes, scanning laser velocimeters, frequency shift, laser diode array, backscatter, forward scatter, light burst, counter processor, fast Fourier transform

19. ABSTRACT (Continue on reverse if necessary and identify by block number)

The feasibility of developing a scanning laser velocimeter (LV/S) for flow measurements in coastal waters and the marine atmospheric boundary layer was investigated. The LV/S, based on a field-proven diode laser Doppler velocimeter (DLDV) for ocean deployment under ice floes, will be designed for backscatter operation. The Phase I investigation has led to the adaptation of a laser diode array rather than a single-element laser diode operating in a pulsed mode, as was originally proposed. At present, the coherence length and pulse width of pulsed laser diodes, which were the two major concerns of the Phase I work, are too short to be suitable as the light source of conventional LDVs. The availability of a high-power laser diode array (up to 5 W) allows operation of the laser diode in the continuous-wave (CW) mode, significantly reducing the potential complexity in the design of signal processors. The

(Continued on reverse)

20. DISTRIBUTION/AVAILABILITY OF ABSTRACT ☒ UNCLASSIFIED/UNLIMITED ☐ SAME AS RPT. ☐ DTIC USERS	21. ABSTRACT SECURITY CLASSIFICATION Unclassified
22a. NAME OF RESPONSIBLE INDIVIDUAL Alan Brandt	22b. TELEPHONE (Include Area Code) (202) 696-4025 22c. OFFICE SYMBOL N00014

19. ABSTRACT (Continued)

scanning diode laser array velocimeter (DLAV/S) will measure profiles of mean and fluctuating flow components as well as wind shear. For measurements in seawater, a diode-pumped YAG laser at 532 nm is a good alternative light source due primarily to its extremely low attenuation, compared to that of diode lasers at 800 nm. Because laser anemometry is also capable of measuring particle size distribution and number density, simultaneous measurements of particle speed, size distribution, and number density may be made with the LV/S. A scanning optical system will be designed for scanning the focal volume, with ranges up to 3 m. During Phase II, test models will be designed, assembled, and tested, leading to the development of a prototype device for field deployment.

ACKNOWLEDGMENTS

The author wishes to express his appreciation to Dr. Y. Agrawal for setting up the FFT processor and furnishing useful suggestions throughout the Phase I investigation. Several of his suggestions may lead to more in-depth testing during Phase II. The author also would like to thank Messrs. C. Pottsmith and R. Srnsky for setting up various test configurations and for carrying out the experiments.

TABLE OF CONTENTS

LIST OF FIGURES

1. INTRODUCTION

To improve the development and maximize the utilization of Naval weapons, it is necessary to understand the dynamic processes and the flow structures in the atmosphere, on the ocean surface, and in the ocean water body. Small-scale, high-frequency turbulence is one of the most important but least understood of these flow structures. Turbulence governs all the transport processes, in terms of mass, heat, and momentum, that play an important role in the ocean sciences, including physical oceanography, marine meteorology, coastal sciences, and air-sea interactions. A suitable field-worthy flow instrument with adequate frequency response and spatial resolution for field deployment in water and air is needed to obtain measurements of turbulent transport properties so that we can improve our understanding of these phenomena.

Flow Research, Inc. (FLOW) conducted a Phase I feasibility investigation on the development of a scanning laser velocimeter (LV/S) for measuring spatial or temporal profiles of flows, turbulence, and current/wind shear in coastal waters and the marine atmospheric boundary layer. This development is a natural extension of a diode laser Doppler velocimeter or DLDV (see Section 2), requiring incorporation of a powerful diode laser and a scanning capability with the DLDV. The identification of high-power laser diode arrays has satisfied the first requirement. One of the main Phase I tasks was to design a scanning lens system, to serve both as the focusing and collecting lens, that would project the focal or sampling volume to the point of measurement and collect scattered light from particles passing through the sampling volume. The scanning lens will be controlled by a stepping motor setup calibrated to provide the position of the focal volume. The LV/S will be designed with a range of about 2 to 3 m.

In this report, the Phase I project is documented in full. First, some background information on laser Doppler velocimetry and diode lasers is presented in Section 2. Then, after the Phase I technical objectives are outlined (Section 3), the experimental methods and apparatus used in Phase I are described in detail (Section 4). The results of the Phase I study are presented in Section 5, and conclusions and recommendations are presented in Section 6.

2. BACKGROUND

Laser Doppler velocimeters (LDVs) have been established as one of the most accurate and versatile instruments for nonintrusive velocity and turbulence measurements (Durst et al., 1976). LDVs are superior to many other velocity instruments in terms of wide dynamic range, fast dynamic response, high spatial resolution, linear calibration, stable or nondrifting characteristics, and applicability in air and water. In particular, LDVs are superior to conventional techniques for measuring multiple-phase flows, as in the breaking wave zone where air bubbles are present (Liu and Lin, 1987). The applicability of LDVs, however, is severely limited by their bulkiness and lack of portability.

These disadvantages have been overcome by the recent development at FLOW of a diode laser Doppler velocimeter for field deployment (Schedvin and Liu, 1984; Liu et al., 1985a, 1985b). In the compact DLDV, the bulky and power-hungry gas laser and peripherals of the conventional LDV are replaced by a miniature diode laser and electro-optical components. This development has revolutionized the application of the laboratory-proven laser velocimetry method for field deployment. The DLDV has been successfully field-tested in Arctic waters under ice floes in two oceanographic expeditions (Liu et al., 1985a). Recently, a second-generation DLDV was developed to remove the directional ambiguity of laser anemometry using a position-sensitive or lateral-effect (LE) photodiode (Liu, 1986; Liu and Bondurant, 1988) rather than Bragg cells, another step forward in achieving portability of laser velocimetry for field deployment. In addition, simultaneous measurements of the speed, size, and concentration of particles (sediment or airborne) may be extended in the near future (Durst et al., 1976).

The DLDV has several advantages over the conventional LDV with a gas laser. These advantages, which make the DLDV especially suitable for field deployment, include:

- Compactness and portability: All components of the DLDV are housed in two small water-tight modules, one transmitting and the other receiving (see description in Appendix). The entire volume of the DLDV is smaller than that of an equivalent 5 mW He-Ne laser alone. Further reduction in size may be achieved by incorporating integrated optronics in the design.
- Low electric power consumption: Both the laser diode (the light source) and the photodiode (the detector) are highly efficient and require only low-voltage DC power. They may be driven by batteries, an attractive feature for field deployment [refer to Spectra Diode Labs (1988) manual].
- Ease of operation: The optics in the sensor head are prealigned, and the DLDV is calibrated in the factory. Yearly recalibration may be required to maintain alignment and calibration for optimum operational conditions. Under the backscatter mode, all

the user has to do during setup is to align the optical axis (marked on the sensor head) of the DLDV to the flow component to be measured.

- Long lifetime: The laser diode has an expected life of 20,000 to 50,000 hours. Replacement of the diode laser is a simple task. At present, the optical module of the diode laser (the laser diode, the collimator, and the beam shaper) is assembled as a unit or subsystem. This subsystem can be further miniaturized by using integrated optronics (optics and electronics). Driven by the optical disk and optical communication industries, the pace of the development of new laser diodes is phenomenally rapid.

At present, the laser diode (index guided) of the DLDV operates in a continuous-wave (CW) mode, which has a maximum laser power of 30 to 50 mW at 780 to 830 nm (for those with single transverse and longitudinal modes). Such laser power is not adequate for measurements over a relatively long range (up to several meters), especially when using the backscatter configuration, which is required for a scanning DLDV as was originally proposed in this project. Further innovation will involve either the identification of a powerful laser diode or operation of the diode in a pulsed mode, which has the potential of increasing the peak laser power about 3 orders of magnitude up to several tens of watts.

Two main difficulties must be overcome to enable operation of the laser diode in the pulsed mode. First, the pulse width of the laser diode must be very short (typically shorter than 200 ns) to operate the diode at a peak power significantly higher than its CW counterpart. Second, the spectral width of pulsed lasers now available commercially is relatively broad ($\Delta\lambda > 3.5$ nm), which degrades the coherence length of a CW diode (in the neighborhood of 10 m). A long coherence length is essential to ensure a distinctive fringe pattern at the focal volume of the two intersecting beams.

In general, the 200-ns pulse width would be too short to accommodate the entire Doppler burst signal for the range of speeds to be anticipated. Frequency shifting of one of the crossing laser beams, creating a "running" fringe pattern at the focal volume with a center frequency in the range of 10 to 100 MHz, would be a potential solution to this difficulty. In principle, the "running" fringe pattern would sweep across particles in the scanning path of the focal volume, which effectively increases the pulse width. It would not only solve the short pulse problem, particularly for low-speed measurements, but would also alleviate the directional ambiguity inherent to laser velocimetry. On the other hand, techniques are available for narrowing the spectral width of the pulsed diode emission. For example, the use of narrow optical filters or an etalon tuned to one of the major lines of emission are two such techniques.

3. PHASE I TECHNICAL OBJECTIVES

The overall Phase I technical objective was to determine the feasibility of developing a scanning laser velocimeter (LV/S) for flow measurements in coastal zones and the marine atmospheric boundary layer (see Figure 1).

The key technical issues were to demonstrate:

- o The adequacy of laser power for operating the DLDV in the scanning and backscatter modes. This objective may be achieved by using a powerful laser diode or operating the diode in a pulsed mode to boost the instantaneous laser power.
- o The design of projecting/receiving optical systems capable of scanning the focal volume along the optical path and receiving the scattered light emitted from particles in the focal volume.
- o The capability of hardware/software for processing the data and deriving the velocity components measured at the focal volume.

The Phase I project also involved identification of hardware for implementing the backscatter sensing (such as image enhancement using microchannel plates) and scanning capability and various data processing schemes, including frequency counting, tracking, and photon correlation. The method of photon correlation has been successfully used for long-range wind velocity measurements using a conventional LDV (Durst et al., 1980).

The successful completion of the Phase I work has led to the submittal of a Phase II proposal to the Office of Naval Research for consideration of further research and development. The Phase II effort will lead to the development of a prototype LV/S for field deployment.

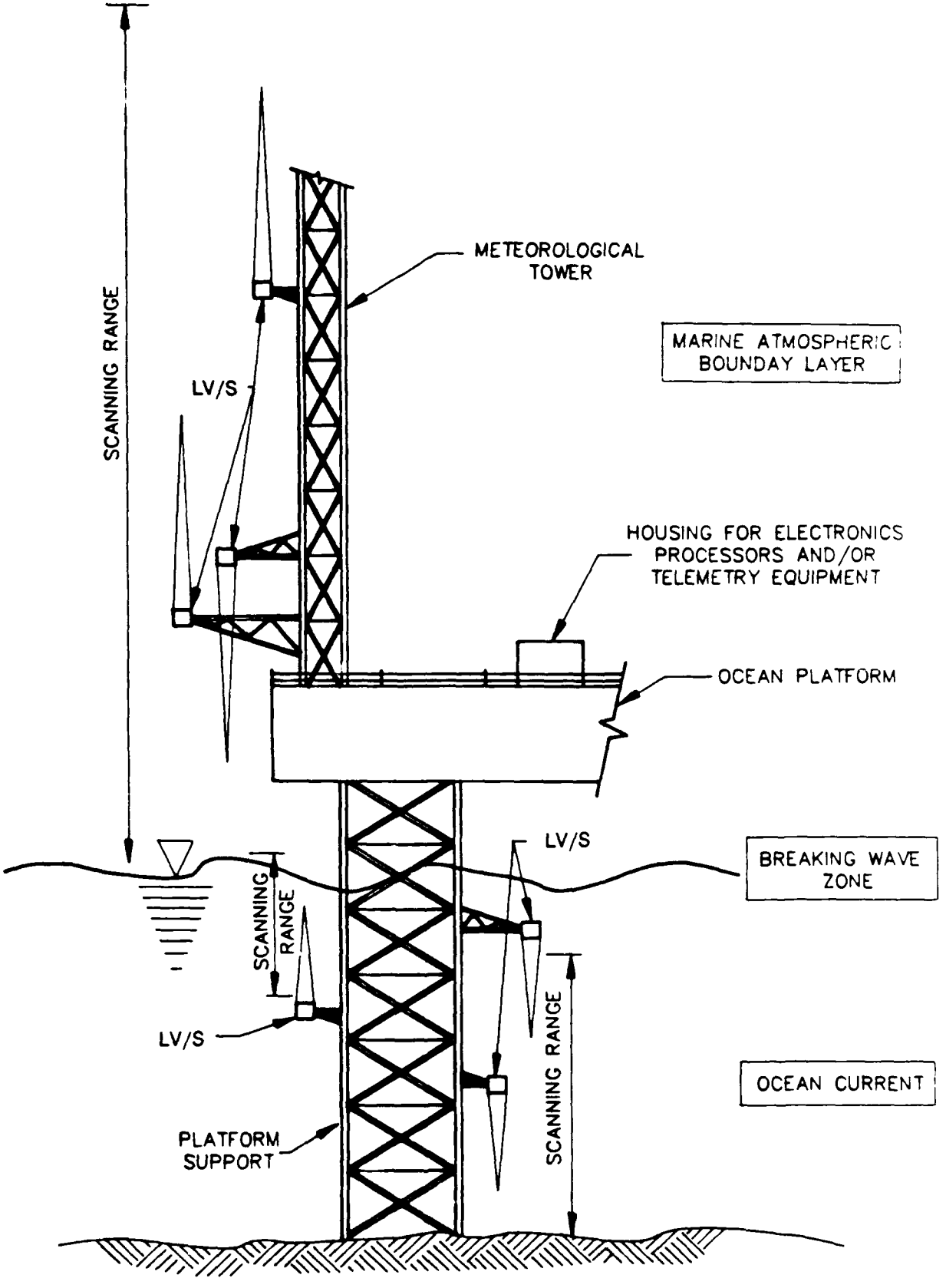

Figure 1. Schematic of LV/S Deployment for Measuring Flows and Sediment/Particles in Coastal and Marine Atmospheric Environments. Rotation of the optics about the optical axis facilitates the measurement of different horizontal flow components.

4. EXPERIMENTAL METHODS AND APPARATUS

The Phase I approach involved the design, fabrication and testing of laboratory models of key LV/S components to demonstrate the feasibility of the proposed research and development. In this section, we describe the experimental methods and apparatus used in the Phase I investigation.

Most of the groundwork for the proposed development of an LV/S was conducted previously through the development of two generations of DLDVs (Schedvin and Liu, 1984; Liu et al., 1985b; Liu, 1986) at FLOW (see Appendix). Thus, the Phase I R&D required essentially an upgrade of the DLDV by incorporating the scanning capability, which also requires a significant increase in the laser power. A natural extension would be to replace the CW laser diode with a pulsed one that could achieve a peak laser power about 3 orders of magnitude higher than the CW counterpart. An alternative would be to use a high-power laser diode that is capable of generating several watts of laser power, such as a multistripe diode array. The optical characteristics of the multistripe diode, however, are different from those of the single-stripe laser diode. Special optronic hardware would be required to utilize the powerful multistripe laser diode as the light source of the LV/S.

In this section, we first provide some technical information regarding the DLDV developed at FLOW. We then review the pulsed DLDV concept, followed by a discussion of the diode laser array velocimeter concept. This section also contains summaries of the scanning lens and data acquisition and processing systems.

4.1 Diode Laser Doppler Velocimeter (DLDV)

Figure 2 shows a schematic of the DLDV operating in the on-axis forward-scatter mode (Liu et al., 1985b, 1989). It consists of a transmitting module and a receiving module. Except for the diode laser, the individual elements are the same as used in the conventional LDV. The

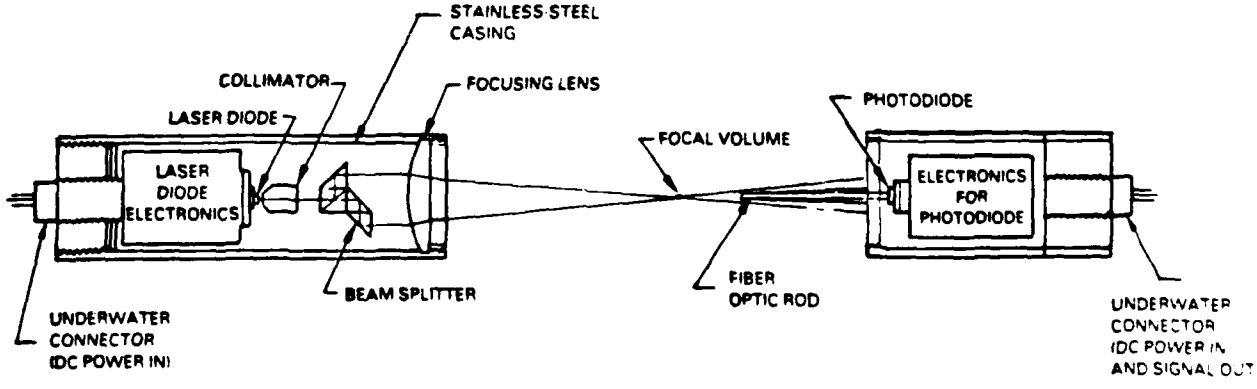

Figure 2. Schematic of a First-Generation DLDV for Oceanographic Deployment (Liu et al., 1985b, 1989)

DLDV was successfully field tested during two oceanographic expeditions for measurements of ocean current and turbulence under ice floes (Schedvin and Liu, 1984; Liu et al., 1985b).

Figure 3 shows a comparison of current measurements made using the DLDV and a propeller current meter deployed in close proximity during the 1984 Marginal Ice Zone EXperiment (MIZEX 84) (McPhee, 1985). The two time series of velocity components measured by the two instruments generally show good agreement. Small-scale deviations are due to a 50-cm vertical separation between the two sensors inside the oceanic boundary layer, the DLDV being at 2.5 m and the current meter at 2 m below the bottom of the ice floes. For a brief description of the first-generation DLDV, refer to the Appendix. For long-range wind speed and turbulence measurements, the DLDV has to be operated in the on-axis backscatter mode, as diagrammatically shown in Figure 4. In general, the intensity of backscattered light is about 3 orders of magnitude lower than that of forward-scattered light. Together with long-distance optical pickup, such a system results in low scattered and detected light powers. To maintain a reasonable signal-to-noise ratio (SNR) for detecting the Doppler frequency from the light scattered by particles passing through the focal volume, several measures may be taken: (1) increase the laser power, (2) improve the sensitivity of the photosensors, or (3) optimize signal processing.

To demonstrate the long-range LDV capability, Durst et al. (1980) deployed a system using a CW 5-W argon-ion laser at 514.5 nm to measure wind speed at 80 and 105 m away from the transmitting/receiving optics. Good agreement was obtained between the LDV measurements and those of a sonic anemometer placed side by side with the focal volume of the LDV (see Figure 5). For a single-mode (in the parallel and perpendicular directions) laser diode, which may be used as the light source of the LDV, the maximum CW power is 30 to 50 mW. This power level is definitely too low for the intended long-range, backscatter wind measurements. When operating in the pulsed mode, however, the peak power of the laser diode may significantly increase, by a factor of up to 3 orders of magnitude of the CW power, provided the duty cycle is low (1% or so). An obvious remedy is therefore to operate the laser diode in the pulsed mode.

4.2 Pulsed LDV

Laser diode pulsers are commercially available to generate laser pulses with a width of 200 to 500 ns, and new pulsers that can generate pulse widths of 500 ns to 10 ms have just recently become available (Power Technology Inc.). The maximum pulse rate is as high as 106 pulses per second. The peak power is inversely proportional to the square root of the pulse width up to 1 ms, beyond which the diode approaches the CW mode. For example, for a diode rated at

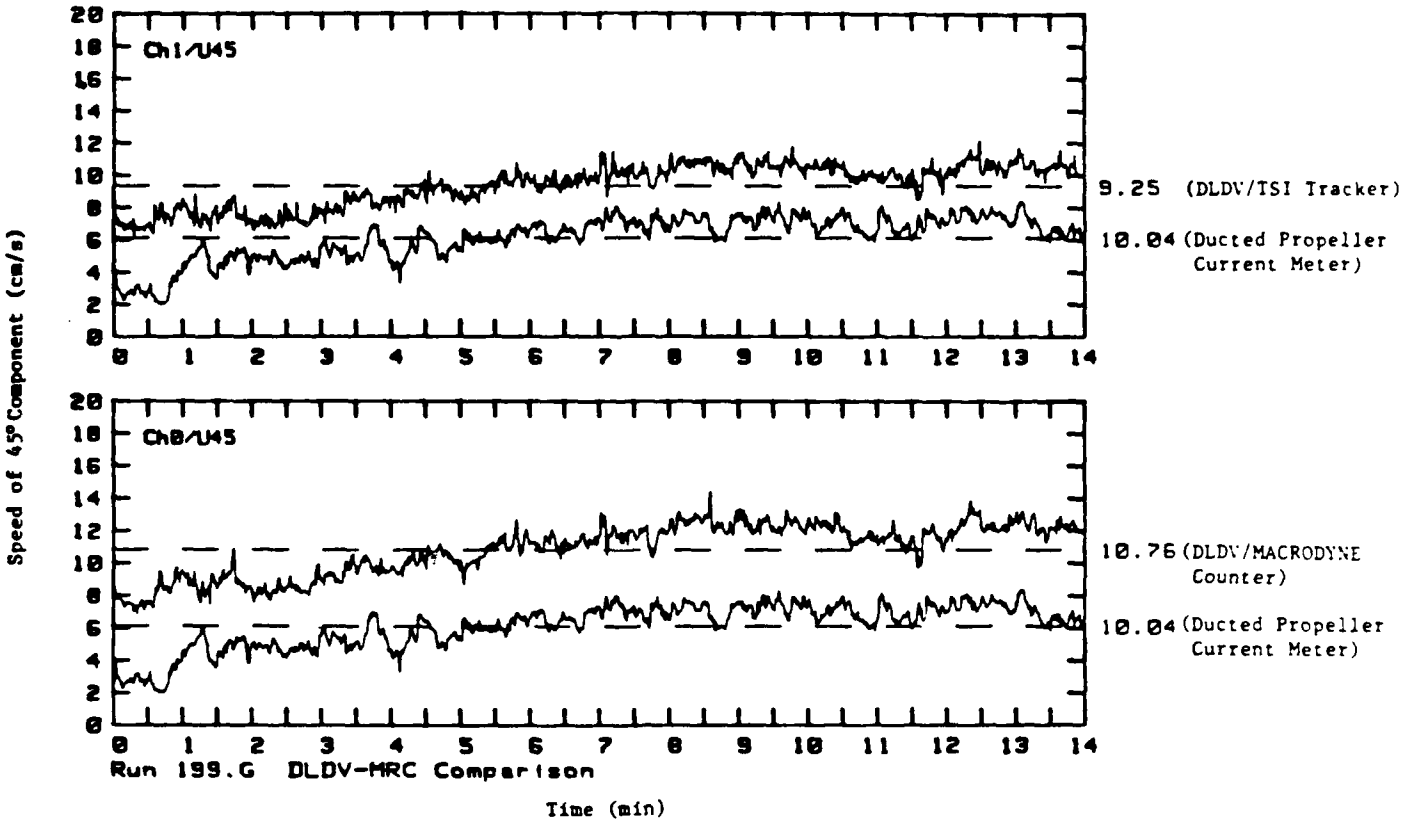

Figure 3. Comparison of DLDV and Current Meter Measurements for the 45° Velocity Component (McPhee, 1985; Liu et al., 1985b). The current meter data are shifted 4 cm/s downward.

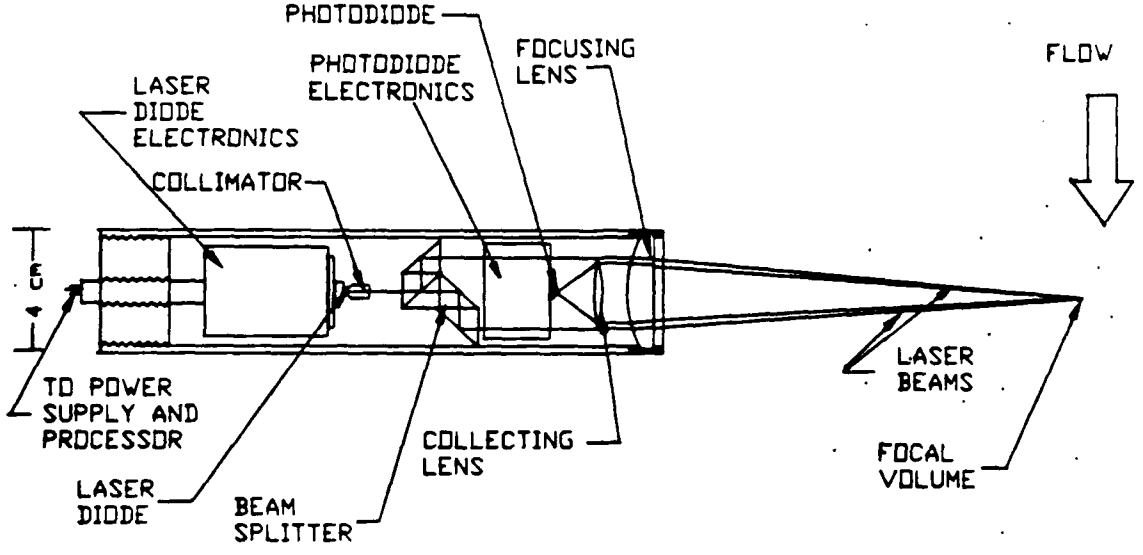

Figure 4. Schematic of a DLDV in a Backscatter Configuration

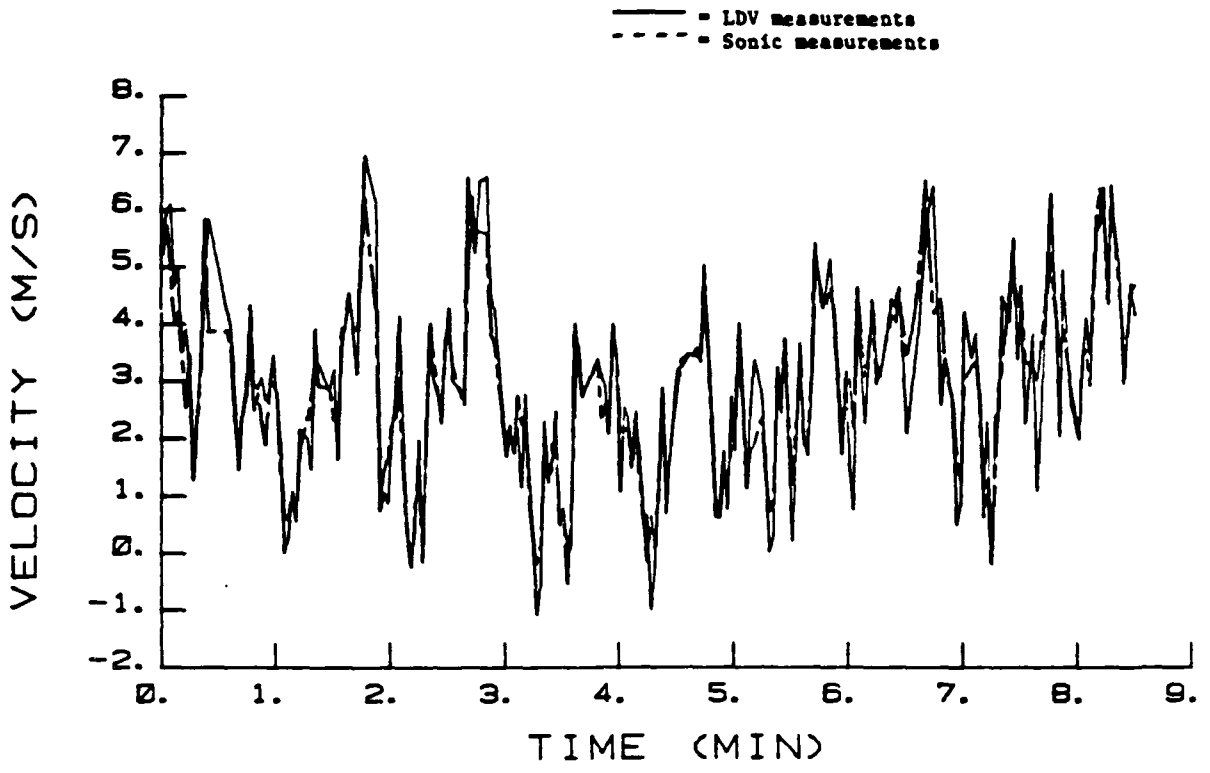

Figure 5. Comparison of Wind Speeds Measured with an LDV and a Sonic Anemometer (Courtesy of Professor F. Durst). The focal distance is at 105 m.

10 W at 200 ns, the peak power at 1 ms would be about 4.5 W. To achieve high peak power, one has to operate the diode at a short pulse width, which would present a different problem. At 500 ns, for example, during any one "on" cycle of the pulse operation, no more than 10 Doppler cycles can be captured for Doppler signals with frequencies lower than 20 MHz. As a result, wind speeds (typically 20 to 40 m/s and lower) corresponding to Doppler frequencies of 20 MHz or lower cannot be measured when the pulse width is set to 500 ns or longer, severely limiting the dynamic range of the system. A remedy for this problem is given below.

Reduction of Spectral Bandwidth

One of the major obstacles for using a pulsed laser diode is that the pulsed emission has several side bands on each side of the major line(s). This results in degradation of the coherence length and potential smearing of the contrast of the fringe pattern. The longer the coherence length, the larger the scanning range, provided that attenuation of the laser light is not significant. Potential remedies are the use of either narrow bandwidth optical filters or an etalon tuned to one of the major lines, with the sacrifice of a reduction in the instantaneous laser power. Optical filters with a bandwidth of 1 nm are commercially available; further

narrowing of the bandwidth can be achieved by using two filters with overlapping windows. In Phase I, we examined these two methods and determined whether they would be suitable for the intended application.

Optical Modulation

An ultimate solution to the limitation of the dynamic range due to short pulse widths would be to shift the frequency of one of the beams by an amount of about 30 MHz, creating a "running" fringe pattern at the focal volume. This is essentially the same as the Doppler-shifted LDV setup using a Bragg cell to remove the directional ambiguity of the LDV. As a result, light scattered from a stationary particle inside the focal volume would have a Doppler signal with a frequency of 30 MHz. Positive and negative (180° difference) wind components will cause the Doppler frequency to increase and decrease accordingly. The maximum negative velocity component resolvable by the system is that corresponding to a Doppler frequency of 30 MHz. In other words, this remedy not only solves the short pulse problem but also removes the directional ambiguity, which is definitely a welcome solution. At present, acousto-optical modulators or Bragg cells are used for the frequency shifting for LDV applications. To be compatible with the portability and compactness of the DLDV, we may look into using electro- and magneto-optical modulators that are small in size and consume low electrical power.

4.3 Diode Laser Array Velocimeter (DLAV)

As mentioned earlier, the maximum power currently attainable for a single-element, CW, index-guided laser diode is 30 to 50 mW. A breakthrough increase in the laser power for this type of diode is not anticipated in the near future due to limitations of the optical power density (106 W/cm^2) at the diode facet. Catastrophic facet damage results when the steady-state optical energy density at the output facet exceeds this limit. This damage melts the mirror facet and causes lasing to cease. Larger apertures permit higher power output without exceeding the facet damage threshold. However, emitters with active region dimensions greater than about 10 μm tend to fail prematurely due to uncontrolled filamentary lasing at high local energy densities and subsequent local facet damage. The creation of multiple coherently (or phase-) coupled small emitters into a multistripe array is a simple process that eliminates filamentary lasing and permits high total power from a coherent source. Optically, multistripe arrays are identical to other geometries of similar aperture. The relatively large aperture of these diode arrays is, however, not suitable for the conventional LDV configuration, such as the crossed-beam differential configuration.

It is important to point out that the near-field pattern of the multistripe diode array depends on the output power. For an array with power below 200 mW, the near-field displays

a number of intensity peaks that, depending on the distance between and size/form of the individual stripes, show very pronounced maxima. Figure 6 shows the typical near-field real fringes of a 200-mW, 10-stripe laser diode array from Spectra Diode Labs (SDL-2420-H1). The basic idea is to bring this near-field distribution in the form of real fringes to focus in the sampling volume for measuring the velocity components of particles passing through that volume. High-quality focusing or imaging optics are required to limit the real fringes in the y-z plane (perpendicular to the axis of the laser light beam). Due to the coherence of the phase array, the real fringe pattern is also spatially limited in the x direction along the laser beam. As a result, a well-defined sampling volume is attainable. This type of laser velocimeter is often referred to as a laser array velocimeter (LAV) (Dopheide et al., 1988). Thus, to be consistent with our convention, we have chosen to refer to it as the diode laser array velocimeter (DLAV).

Several types of optical systems for forward scattering and backscattering have been tested by Dopheide et al. (1988). They also presented a case for directional sensing by masking one of the stripes of the array. Their methods are only applicable to relatively low power diode arrays with a distinctive near-field real fringe pattern. For high-power laser diode arrays (> 200 mW),

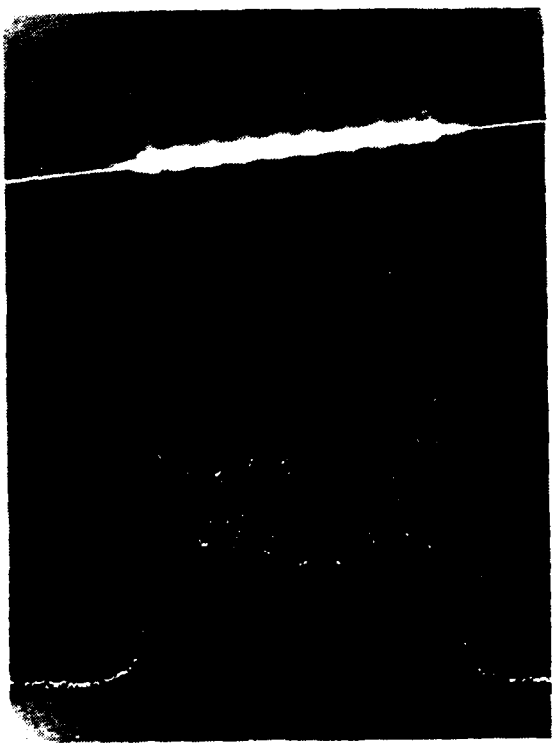

Figure 6. Near-Field Distribution of a Phase-Coupled Laser Diode Array (SDL-2420-H1 with a maximum power of 200 mW)

the distinctiveness of the real fringe pattern reduces with increasing laser power. For laser diode arrays with power exceeding 1 W, the near-field pattern becomes a nearly uniform "top hat" distribution. Our main interest here is the high-power diode array for scanning operations.

4.4 Scanning Lens System

To project the focal volume to the measuring points and to collect onto the photosensor the scattered light from particles passing through the focal volume, a special scanning lens system is required for relatively short distance projection and collection. This scanning lens system, which replaces the front lens as shown in Figure 2, will be equivalent to a telephoto lens for photography. The design of the scanning lens system depends on the configuration of the optronics that forms the focal volume. During Phase I, a simple model of the scanning lens system was designed, assembled and tested with the DLAV/S laboratory model for the feasibility investigation. The Phase I findings will lead to the design and fabrication of a sophisticated scanning optical system for projection of the focal volume and collection of the scattered light in Phase II. The scanning assembly will have an LVDT output to monitor the position of the focal point at all times during data acquisition for reconstruction of the wind or wind shear profile. Again, portability and compactness will be major considerations in the design of the scanning lens system.

Enhancement of the sensitivity of the photosensors may be made by the incorporation of an image intensifier such as microchannel plates, if needed. Miniature, highly sensitive image intensifiers (with a 10^6 gain) are now commercially available (e.g., Hammamatsu Model V2025). Such an incorporation would definitely enhance the photon correlation method. It is plausible that the image intensifier provides so much gain that the conventional counter processor is adequate, at least for a medium range of scanning. During Phase I, we further investigated the application of image intensifiers for the proposed development.

4.5 Data Acquisition and Processing

We anticipate that the signals from the prototype DLAV/S may require advanced processing algorithms, such as photon correlation (Durst et al., 1980), for on-line data analysis (Sharpe, 1979). Such a signal processor would include a high-speed digital correlator and an 80386-based PC to perform real-time fast Fourier transforms (FFTs); the peak of the FFT results corresponds to the dominant frequency of the scattered light signals and, therefore, the magnitude of the flow components to be measured. For example, TRW has made available an FFT chip that is capable of performing FFTs at very high speeds. The FFT chip would definitely enhance the real-time photon correlation method. Implementation of photon

correlation hardware and software, if required, will be made during Phase II. The 80386-based PC will serve as a stand-alone data acquisition and analysis system. Data recorded with the system may be uploaded to mainframes for high-speed data analysis.

Nicolet Digital Oscilloscope

The Nicolet 4094 digital oscilloscope consists of three main components: the mainframe, the Model 4562 plug-in, and the XF-44/1 disk recorder. The mainframe includes a display memory, display screen, and various controls to manipulate the display screen components. The controls feature horizontal and vertical expansion to x256, autocentering, choice of XY and XT displays, 16K word display memory that can be left intact or divided into halves or quarters, and multiple function abilities including arithmetic manipulations, electronic graticule, and pen recording outputs.

The Model 4562 plug-in includes two 12-bit, 500-nanosecond digitizers. Other features include two high-impedance differential amplifiers; single 16K word memory; single-ended or differential amplifiers; positive, negative, or dual-slope triggering; normal trigger, pre- and post-trigger, and delayed trigger displays; a trigger view mode for setting up the triggering threshold; low-pass filtration; and sweep and point averaging.

The disk recorder transfers data onto the floppy diskette for storage. The stored data can be recalled at a later time for inspection on the screen. The diskette is divided into 20 individual records, each capable of storing either one (16K), two (8K), or four (4K) data groups. A set of 23 programs is available for statistical and waveform analysis of the signals stored on diskettes. For example, there are programs to estimate the maximum and minimum values, the rise time of a wave form, the area, and the average and rms values. Programs are also available for differentiation, integration, and inversion of the signals. The stored data may be transferred to the PC for further analysis and may also be displayed graphically.

For the Phase I investigation, we used two types of processors available at FLOW: the counter-type and FFT processors. The counter processors include a Macrodyne Model 2096 processor and FLOW's DLDV/DS processor (Liu and Bondurant, 1988).

Data Acquisition System

The DLDV/DS is equipped with an on-line data acquisition system (DAS). To assist with the development of the DLDV/DS system, an AT-type personal computer (PC) was used to collect and analyze data from the DLDV/DS unit. A 64-bit wide parallel interface was used to handshake information from the DLDV/DS unit to the PC. The sampling frequency of the PC was controlled by the DLDV/DS unit via one of its 64-bit parallel outputs. This bit was

brought to an active state every time a data block was ready. The actual sampling frequency was sent to the PC via four binary-coded decimal (BCD) values. The largest value that the system was capable of sending was 999.9 hertz.

Other information collected by the computer include the highest burst frequency that was detected over the last sample period (and the channel that detected the burst), the exact position in that time interval that the burst occurred (burst location), and the direction of the burst. All this information was collected and stored in the computer's memory during a data collection run. Once the information was collected, it could be saved to disk for future retrieval and was also available for the operator to review.

During a review process, selective information could be written to the disk in a format compatible with other spreadsheet software packages. In addition, the program could calculate the mean and standard deviation for a given data set and display the number of readings that were made on each of the individual channels. Another option allowed the operator to store to disk only data that was valid (indicated by a valid channel number). This was needed in order to reduce the amount of information that was stored when very low particle counts were present in the sensing area.

In order to collect information from the DLDV/DS, the following hardware is needed:

- o AT-type computer
- o Burr-Brown Base Module with 32 bits of Parallel I/O PN# PCI-20001C-2 Base Address CF00H
- o Burr-Brown 32-bit Parallel Expansion Module PN# PCI-20004M-1 Expansion Slot\ 3
- o JRAM-AT3 memory card with 2 Mb Memory Bank Select Register E800:0000 Mapped Page for memory access D000:0000

If a review of an old file is needed, only the AT computer and the JRAM are required.

The operation of the program is controlled with the use of menus. The Tab and Shift-Tab keys are used to highlight the different menu items. Selection of a highlighted menu option is done with the Enter/Return key. The first time the program is run after computer power-up, it is essential that the JRAM memory be initialized. This is accomplished by first selecting the "Modify Parameters" option which is found in the top-level menu, and then selecting the "Init Ram" option. This will cause the computer to test and initialize the memory used by the system. Once this is completed, return to the top-level menu and proceed with another option. The system menu options include "Gather Data," "Review Data," "Modify Parameters," "Convert File" and "Save Data." In addition, we used several software packages such as the LOTUS 123 spreadsheet by Lotus Corporation, Asystant Plus by Macmillan Software

Company, MATLAB by Math Works, Inc., and SIGMAPLOT by Jandel Corporation. These packages include all the statistical and spectral analysis routines required, together with graphics, for the reduction and analysis of the experimental data.

FFT Signal Processor

The FFT signal processor was developed by Agrawal and Belting (1988) and is based on a Fourier transform method (Agrawal, 1984). This processor continuously sweeps across the spectrum of the incoming signal. The frequency containing the spectral peak is saved and presented as the velocity data. This approach has the twin advantages of being completely insensitive to signal drop-out (as against phase-locked-loop trackers) and being ideal for low SNR applications (unlike the counter processor, which is suitable for intermittent signals but requires high signal quality). The processors have been used in the deep sea (Agrawal and Belting, 1988) and in shallow water (Agrawal et al., 1988). The former application exemplified a low-data-rate situation; the latter, a continuous-signal situation. The same principle has been applied in more recent commercial LDV processors, but they are also an order magnitude more expensive.

The processor consists of a modified chip-Z FFT signal processing board (Reticon-5601) and circuitry to extract the frequency at the spectral peak. The frequency resolution and data rate are related by the fundamental relationship $\Delta f\ (\Delta t/2) = 1$, where Δf is the frequency resolution (8 bits) and Δt is the sampling interval. The factor 2 enters due to the use of only half the spectrum as the second half (from f_N to 2 f_N, where f_N is the Nyquist frequency) is a reflection nearly 0.5 kHz. Tests were conducted in Phase I using the DLAV configuration to determine the performance of the FFT processor for analysis of the backscattered signals. An attempt was made to identify some hardware that would miniaturize the processor for field deployment. The SNR level at relatively short scanning distances was determined. The SNR for long-range scanning will be extrapolated as the basis for the prototype development in Phase II.

4.6 Flow Facilities

For tests of the DLAV model in air, we used an air jet by fitting a nozzle of 1 cm diameter to the outlet of an ultrasonic humidifier (Gemtech Model AH-1501). Water droplets generated by the humidifier are excellent seeds for laser velocimeters. Refer to Liu and Bondurant (1988) for a detailed description of the facility and other peripherals designed to control the number density of water droplets in the air stream.

During Phase I, we tested the DLAV model with the use of DLDV/DS receiver and the directional counter processor to demonstrate the directional sensing capability of using an LE

photodiode (Liu and Bondurant, 1988). A series of tests was conducted in an oscillatory flow facility consisting of an air cylinder driven by a crank motor. The air cylinder is connected to a square vertical pipe (5.08 cm x 5.08 cm) with two optical windows made of microscope plate glass for the passage of the laser beam and viewing of the sampling volume. The pipe was filled with tap water (through a 10-μm filter). The water column in the pipe undergoes an oscillatory motion when the crank motor is turned on, as water is forced into and out of the air cylinder. The rotational speed of the motor controls the frequency, and therefore the speed, of the oscillation.

5. PHASE I RESULTS

In this section, we present the Phase I results derived from a literature review and laboratory experiments. These results are further analyzed to determine the feasibility of the proposed development of a scanning DLAV.

5.1 Pulsed DLDV

As originally proposed, we first designed and assembled a test model of the DLDV using a pulsed laser diode for the Phase I feasibility investigation. One of the most important tasks was to determine whether the optical characteristics of the pulsed diode lasers, in terms of the peak laser power, the coherence length, and the maximum pulse width, are suitable for incorporating the scanning capability in the DLDV.

As a part of Task 1, we purchased two pulsed laser diodes from Laser Diode, Inc. (Models LD-62 and LD-63). The diodes emit near infrared light with a nominal wavelength of 904 nm, which is only visible by the naked eye via a fluorescent screen or viewer. They were driven by a power supply specifically for pulsed operations (Power Technology, Inc., Model IL20C100/200PSV). The maximum repetition rate and pulse width are 10 kHz and 200 ns, respectively. The maximum instantaneous power that decreases with increasing pulse width is about 6 to 7 W. At a pulse width of 200 ns, the instantaneous power reduces to about 1 to 2 W.

To form the focal volume in the cross-beam differential or fringe mode, we placed a diode laser collimator in front of the diode to create a collimated beam. The beam was then split into two parallel beams, using a 1-cm-cube beam splitter, and then these beams were passed through a focusing lens. The focal volume was imaged and magnified on a screen by using a 40x microscope objective. A fringe pattern would be formed on the screen, as in the case for the CW setup, provided the coherence length of the pulsed laser was longer than the difference in the optical path through the beam splitting and focusing optics. A clear image of the fringe pattern is essential for the cross-beam LDV to work properly.

No fringe pattern was observed when we set up the above configuration. After an extensive discussion with the manufacturer, we learned that the coherence length of the pulsed diode, in its current configuration, is at best 0.5 mm. Such a coherence length is practically too short for the intended applications, especially for a relatively long-range projection and pickup for a scanning LV. For comparison, the coherence length of a CW index-guided GaAlAs laser is on the order of several meters. In an attempt to improve the coherence length of the pulsed diode, an interference filter centered at 904 nm with a bandwidth of 3.5 nm was inserted between the laser beam and the optics. Little improvement was observed. We also acquired an etalon with a centered frequency of 904 nm. Although the etalon has higher optical transmission and narrower bandwidth than does the interference filter, no significant difference in

the improvement in the coherence length was observed between the two. Both were considered failures in providing the much-needed bandwidth filtering to improve the coherence length of the pulsed laser diode.

5.2 Diode-Pumped YAG Laser

A second potential light source for the scanning LV for ocean deployment is laser-diode-pumped solid-state YAG lasers (e.g., Amoco Laser Company). At present, commercial microlasers are available for visible (ALC 532, 5 mW) and near-infrared (ALC 1064, 100 mW) emission. Research units with much higher power have been sent out for evaluation. According to Amoco, visible and near-infrared microlasers with CW power up to 100 and 500 mW will be available soon. Note that the attenuation in seawater of the laser light at 532 nm is significantly lower than that at 800 nm; the 50% attenuation lengths for these microlasers are 6.9 m and 0.25 m, respectively. The attenuation length of the green laser is about 2 to 3 times longer than that of a He-Ne laser (633 nm). At present, a 5-mW CW He-Ne laser has been successfully used as the light source for an underwater LDV operating in a backscatter mode (Agrawal and Belting, 1988). A range up to 1 m was achieved. Therefore, a 100-mW green laser (532 nm), which is equivalent to a 3-W near-infrared laser (800 nm) when used underwater, should be adequate for a scanning, backscattering LDV to a range up to about 3 m. Therefore, the diode-pumped solid-state YAG microlasers are potential candidates for the light source for a field LDV if their power achieves 100 mW or higher (Chumbley, 1989).

5.3 Diode Laser Array Velocimeter (DLAV)

The failure of using pulsed laser diodes as the light source for the scanning LV prompted our investigation into the use of high-power CW diode arrays as a potential candidate and, thus, introduced the concept of the DLAV. The preliminary work of Dopheide et al. (1988) has shown encouragement in the proposed R&D. Our Phase II development, however, will be way beyond the power range of Dopheide et al. (1988), in which the ac amplitude modulation of the array disappears entirely. During Phase I, we conducted a series of laboratory experiments and a literature search to further examine the feasibility of developing a scanning DLAV. First, we designed, assembled and tested a laboratory model of a DLAV. Second, we designed innovative optronics for generating the near-field real fringe, whose distinctiveness disappears for a high-power diode array (> 1 W). Finally, we designed a scanning lens system for projecting the real fringe along the optical path of the scanning focal volume and collecting the scattered light signals from particles passing through the focal volumes. In the following, we describe the Phase I R&D activities.

DLAV Laboratory Models

As the light source of the DLAV, we acquired a phase-coupled 10-stripe diode array from Spectra Diode Labs (Model SDL-2420-H1). The maximum laser power is 200 mW at 798 nm. To ensure an optimum near-field distribution of the real fringe pattern (relatively uniform distribution with maximum amplitude modulation), we had the manufacturer hand select from a lot of about 12 diode arrays before packaging the array into the TO-3 canister. There are a total of 10 stripes of emitters with amplitude modulations that are about one-third to one-half of the maximum dc intensity (Figure 6). Note that the ac modulation rather than the dc level contributes to the usable signals for velocity measurements.

Figure 7 shows a schematic of one of the laboratory models of the DLAV. The entire setup was mounted on an optical table. A Liconix LDD100 laser diode driver (1) was used to drive the 10-stripe SDL-2420-H1 diode array (2). A Newport laser collimating lens assembly with an 8-mm focal length (3) was placed in front of the array to project the near-field real fringe pattern to the sampling volume (5). For backscattered light collection, a receiving lens (6) with a focal length of 0.5 m was placed 70 cm from the sampling volume at an angle of 20 to 30° from the optical axis of the DLAV. The first-generation DLDV receiver with the fiber-optic rod (Liu et al., 1985b) was used for collecting the backscattered light onto the photosensor. The output signals were fed into the processors, either the counter- or FFT-type. An air jet with a diameter of 1 cm (Section 4.6) was used to test the DLAV model. Water droplets generated by an ultrasonic humidifier were used to seed the flow.

To facilitate the scanning capability, we added a Melles Griot 06 GLC 006 laser collimating lens assembly (50-mm focal length and 20-mm clear aperture) between the air jet and the first collimating lens (3). For this setup, a relatively small movement of the lens system (3) would result in a large movement of the focal volume along the optical axis of the DLAV. This is an excellent feature when automated scanning is to be implemented in Phase II. The fringe spacing, however, would also increase linearly with the projection or scanning distance from the face of the diode array. Preferably, the fringe spacing should be independent or only weakly dependent of the scanning distance. Innovative design of the scanning optics will be required to achieve this.

It turned out that the SNR from the photosensor output of the DLDV receiver was too low for proper operation of the FFT processor (Agrawal and Belting, 1988). Subsequently, we replaced the DLDV receiver with a photomultiplier made by Hammamatsu (Model R928, range 185 to 930 nm); the photomultiplier has a significant increase in the gain at the sacrifice of the quantum efficiency at 798 nm as compared with the silicon photosensor used in the DLDV receiver.

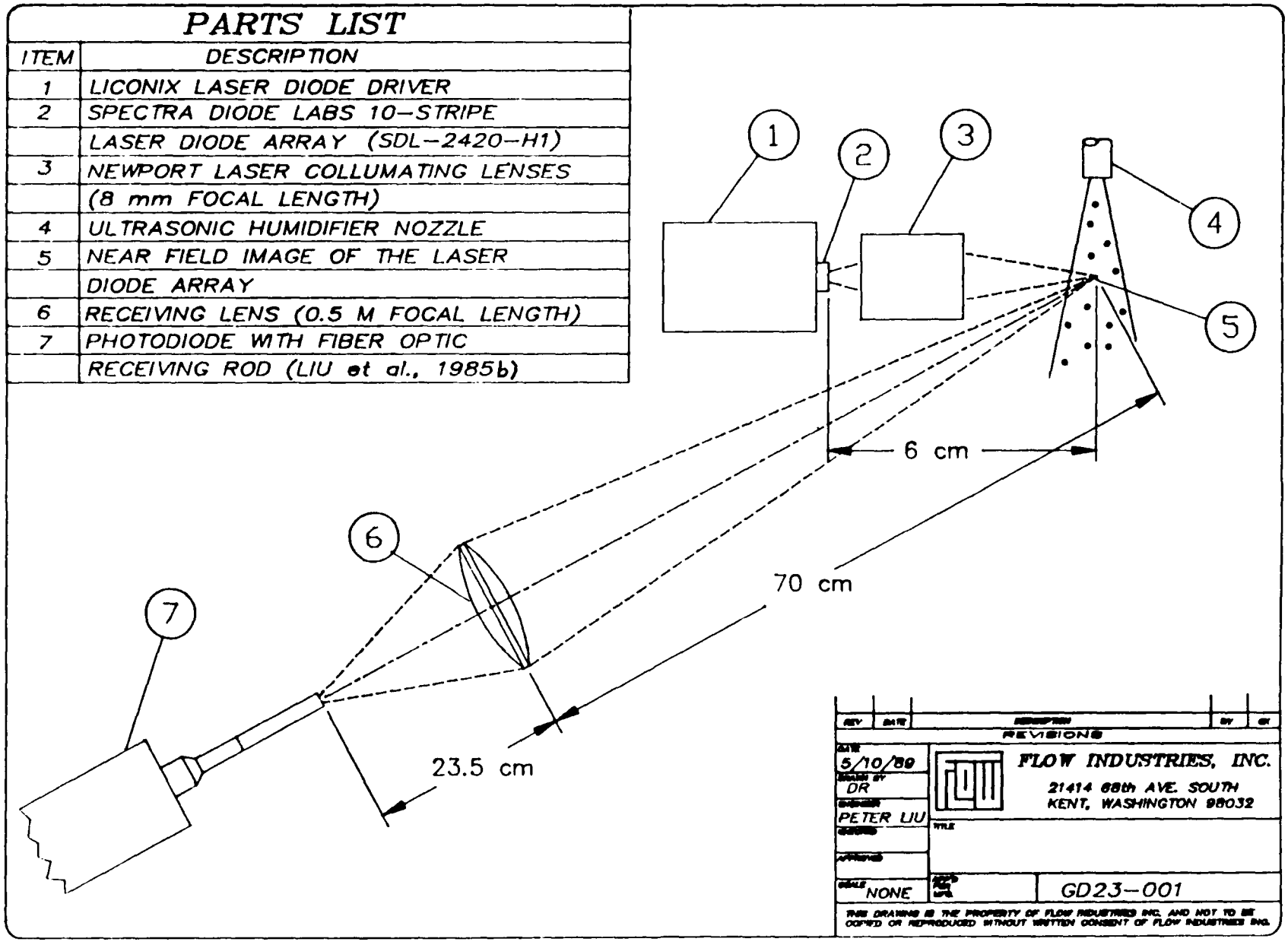

Figure 7. DLAV Laboratory Model

The backscattered signals were first fed through a band-pass filter (Krohn-Hite Model 3103) and then displayed on the screen of a Nicolet digital oscilloscope. The digital signals were recorded on floppy disks and transferred to a PC for storage and further analysis and examination. Figure 8 illustrates a typical light burst scattered from a particle passing through the sampling volume. There are a maximum of 10 alternating dark/bright bands in each burst, resulting from the illumination of the particle by the 10-stripe diode array (Figure 6). Note that the shape of the burst differs significantly from that of the classical Doppler burst (Durst et al., 1976); the latter has many more zero crossings and is more or less Gaussian in distribution. For comparison, the background noise in the absence of a particle in the sampling volume is also plotted in the same figure. Superior SNR is evident from this figure.

Figure 9 shows a typical time series of the output from the photosensor in response to passage of particles in the air jet through the sampling volume at which the near-field real fringes are imaged. There are two pronounced light bursts about 1 ms apart with excellent SNR. These would result in validated velocity measurements after the signals are processed. There are also less pronounced bursts with only 3 to 4 cycles and relatively low amplitude modulation. The weak bursts correspond to signals generated by small particles passing through the edge of the sampling volume at an angle to the optical axis. They will not to be validated when a counter processor equipped with a comparator using 5 (counts)/8 (counts) convention. The dominant frequency of the weak bursts may be determined with the use of an FFT processor; the accuracy would be poor due to too few cycles in the bursts.

Dominant Frequency of Burst Signal

By feeding the time series into the FFT processor, the dominant frequency of the light bursts is determined. Figure 10 shows the time series of the dominant frequency measured with the FFT processor near the exit of the jet at $x/D \sim 2$, where x is the distance from the nozzle and D is the jet diameter. The measured dominant frequencies are consistent with those estimated from the time series of the light bursts recorded with the Nicolet oscilloscope (e.g., Figure 9). For the particular experimental setup, the fringe spacing is about 50 μm. Therefore, the conversion factor is 20 kHz/cm/s. The mean frequency of 25 kHz corresponds to about 1 m/s exit speed of the jet. It is evident that the time series is contaminated by low-speed spikes that have no physical significance. It turns out that the spikes correspond to the speed of some relatively large water droplets, formed as a result of the merging of small droplets, that tend to lag the jet flow. This is confirmed by the slow but continuous accumulation of water inside the nozzle. To remove the contribution from the low-speed, large droplets, we deleted all the data points with speeds deviating more than two standard deviations from the mean

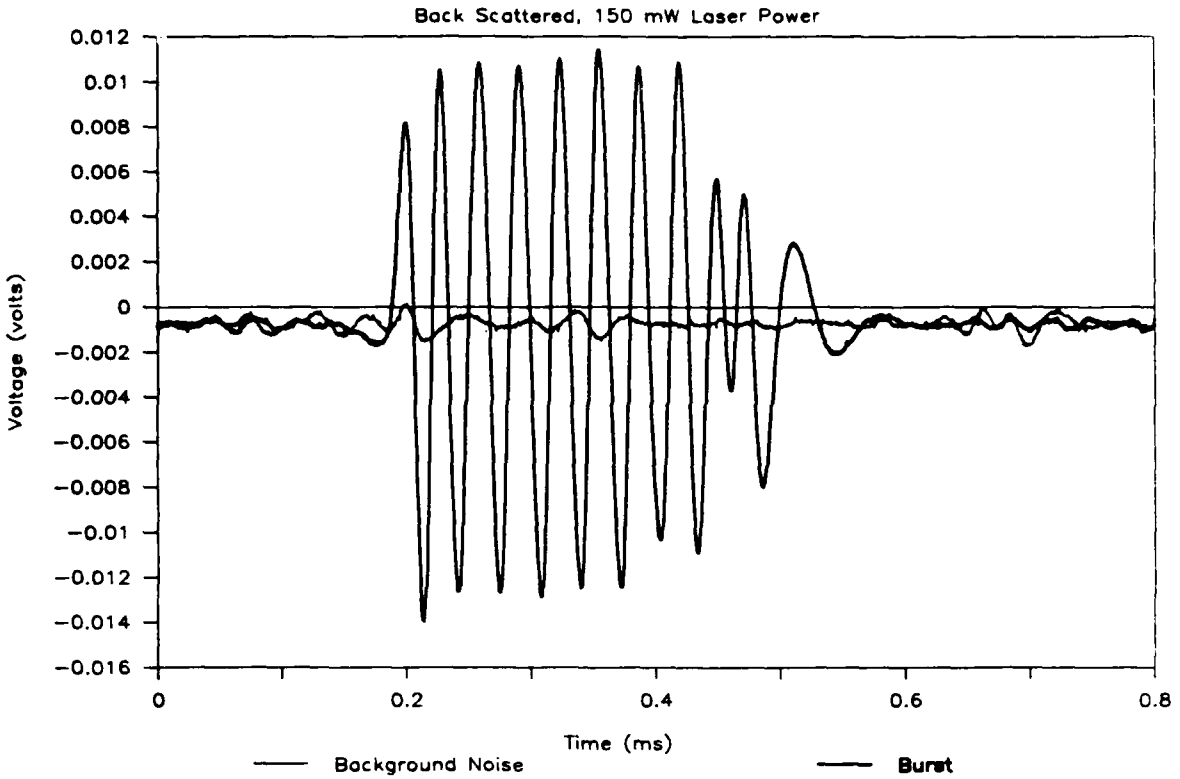

Figure 8. Comparison of DLAV Burst Signal and Noise

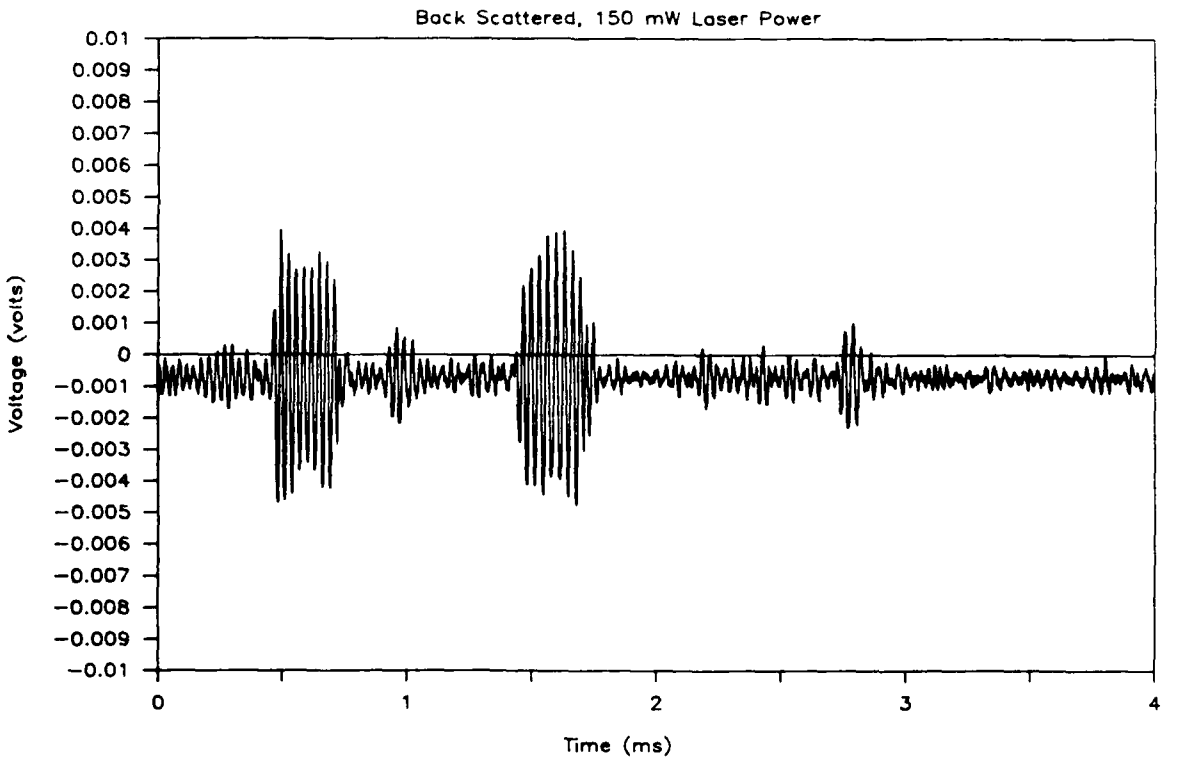

Figure 9. Time Series of Multiple Bursts

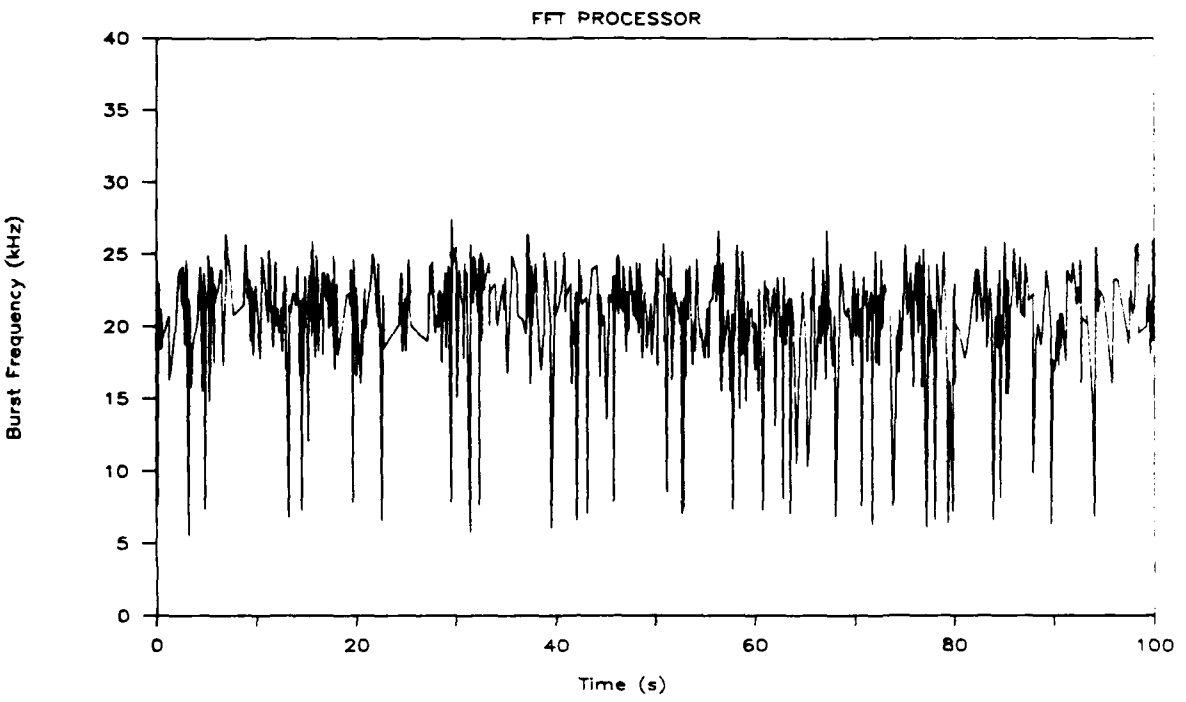

a. 100-second duration

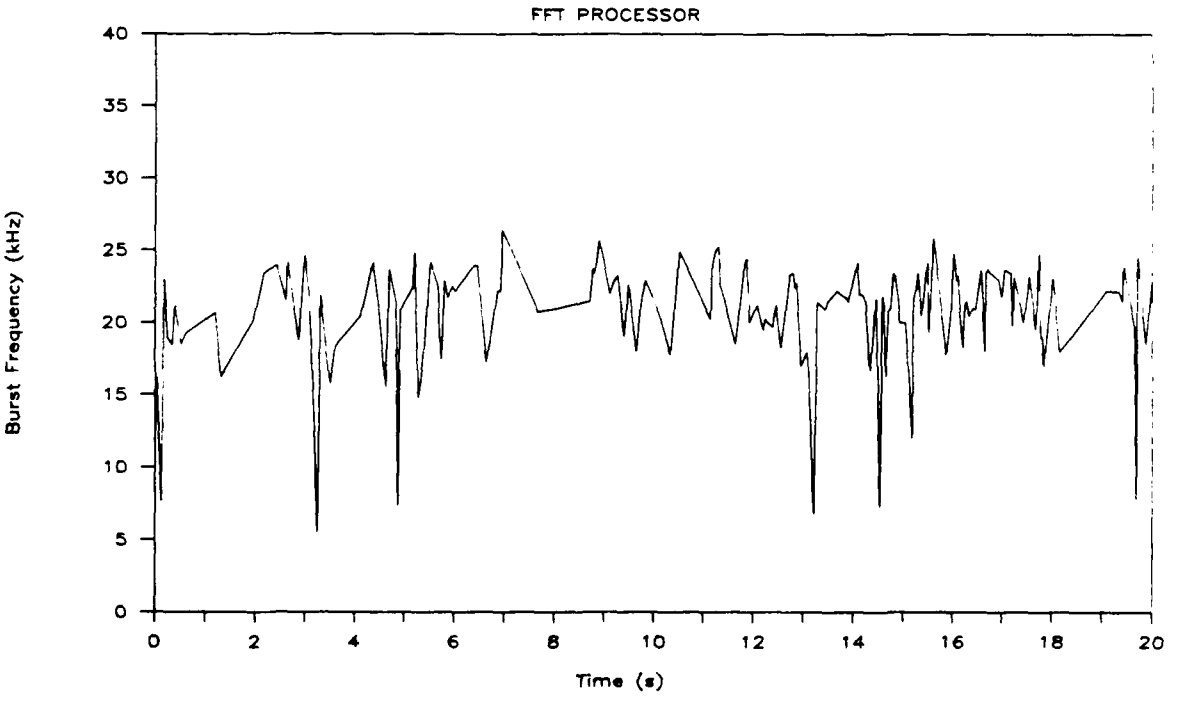

b. 20-second duration

Figure 10. DLAV/FFT-Processor Measurements of the Longitudinal Velocity Component Near the Exit of an Air Jet (1.00 cm diameter). Low-speed spikes are due to large water droplets that impede the air flow.

speed of the jet. The resulting time series is free of the low-speed spikes, as illustrated in Figure 11.

Figure 12 illustrates the time series of dominant frequencies measured at x/D = 20 along the centerline of the jet. It is interesting to point out that the mean speed of the jet reduces to about half of that at the jet exit and the signals are highly intermittent; these are well-known characteristics of a turbulent jet. Also, note that there is no longer the low-speed spikes observed in the time series, as the large water droplets have dropped out from the jet at 20 diameters downstream.

For the 10-stripe diode array used for the DLAV model, the maximum number of cycles for each light burst is 10. Due to the few zero crossings in each burst, the error in determining the dominant frequency of the burst is expected to be relatively high. The cure would be to increase the number of zero crossings, which will be accomplished in Phase II by using a fine grating to create the near-field real fringes.

Directional Sensing

For removing the directional ambiguity of laser velocimetry, we set up the DLAV model together with the directional sensing receiver and processor from the second-generation DLDV/DS (Liu and Bondurant, 1988; Liu et al., 1989). A series of laboratory tests was conducted in a flow facility capable of generating an oscillating water column (see Section 4.6). For this series of tests, we operated the DLAV in the forward-scatter mode (slightly off axis), as the lateral-effect (LE) or position-sensitive photodiode has relatively low sensitivity compared with the photomultiplier used in previous experiments. The sampling volume was imaged onto the surface of the LE diode via the imaging optics of the DLDV/DS receiver. Tap water passing through a 10-μm filter was used as the working fluid. Previous experience has demonstrated that relatively clean water has to be used in the facility to avoid the simultaneous presence of multiple particles in the sampling volume, the main source of error in measuring the flow direction.

During one of the tests, the DLAV was configured to have a fringe spacing of about 35 μm. To demonstrate the directional sensing capability, Figure 13 illustrates two sets of burst and direction signals excerpted from the two outputs of the directional counter processor. In essence, the two outputs are the sum and difference of the raw outputs from the two end terminals of the LE diode. The two sets of signals correspond to the upward (Figure 13a) and downward (Figure 13b) movements of the water column, as represented by the slope of the direction signals designated by the thick solid curves. There is a lag between the burst and direction signals, which is accounted for in the software of the processor.

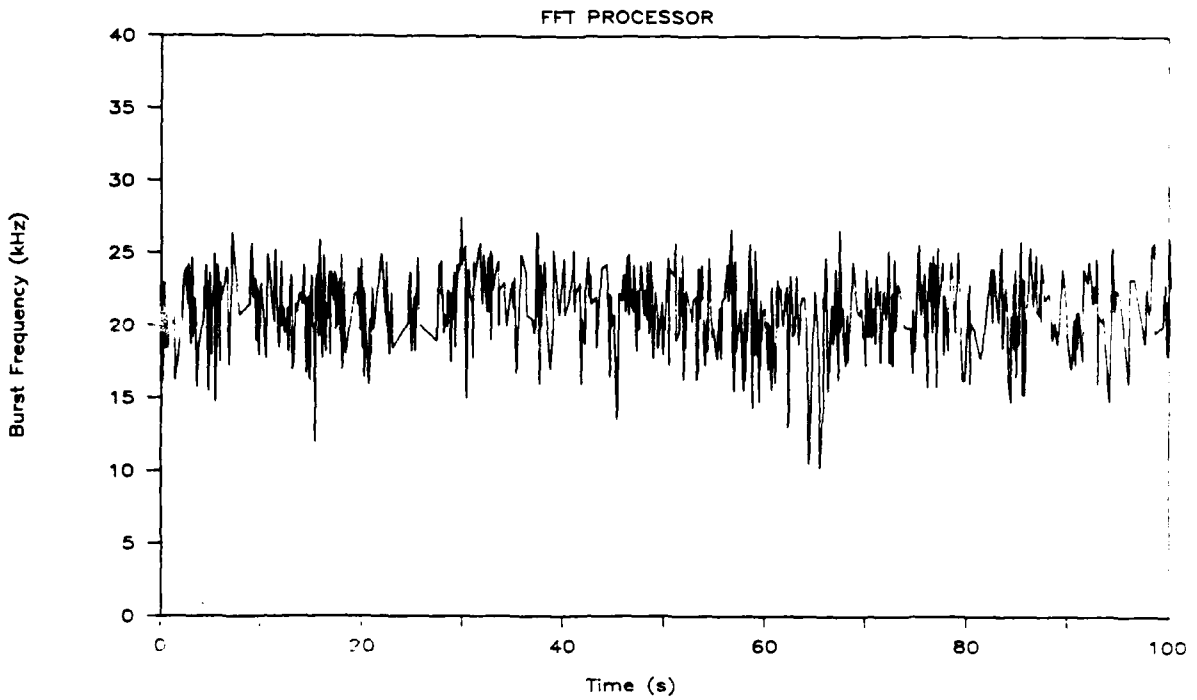

a. 100-second duration

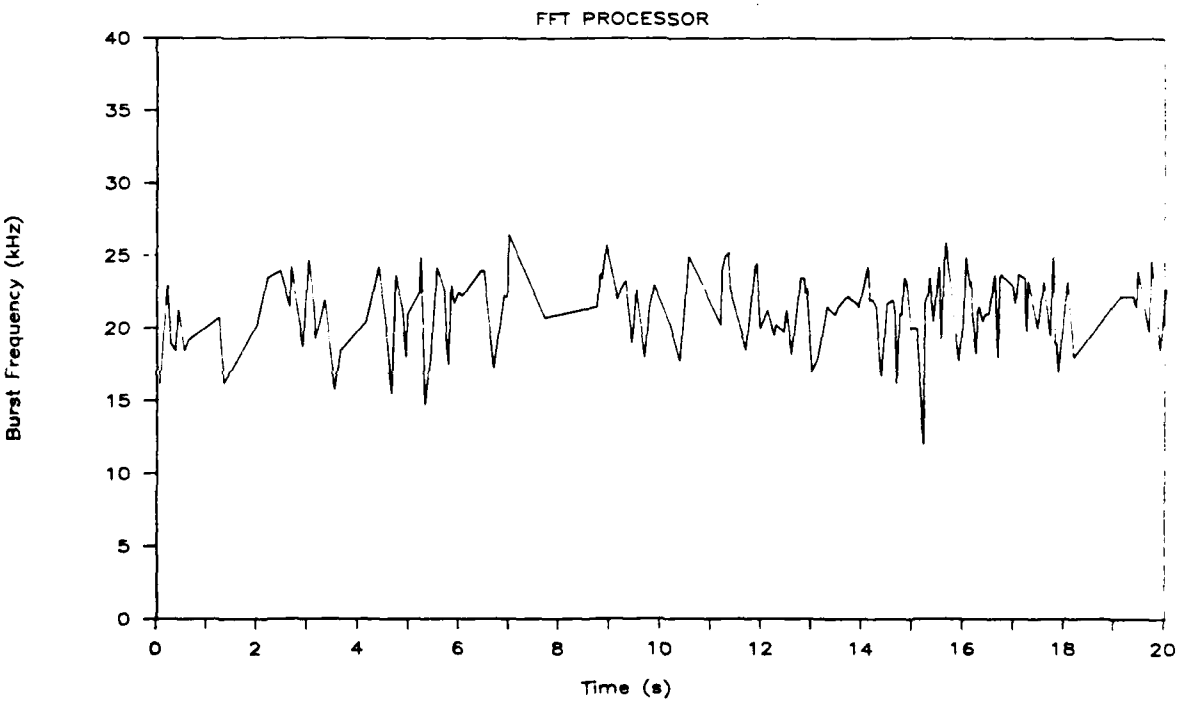

b. 20-second duration

Figure 11. DLAV/FFT-Processor Measurements Shown in Figure 10 Except the Low-Speed Spikes Are Removed by Deleting Data Points with Values more than Two Standard Deviations from the Mean Value

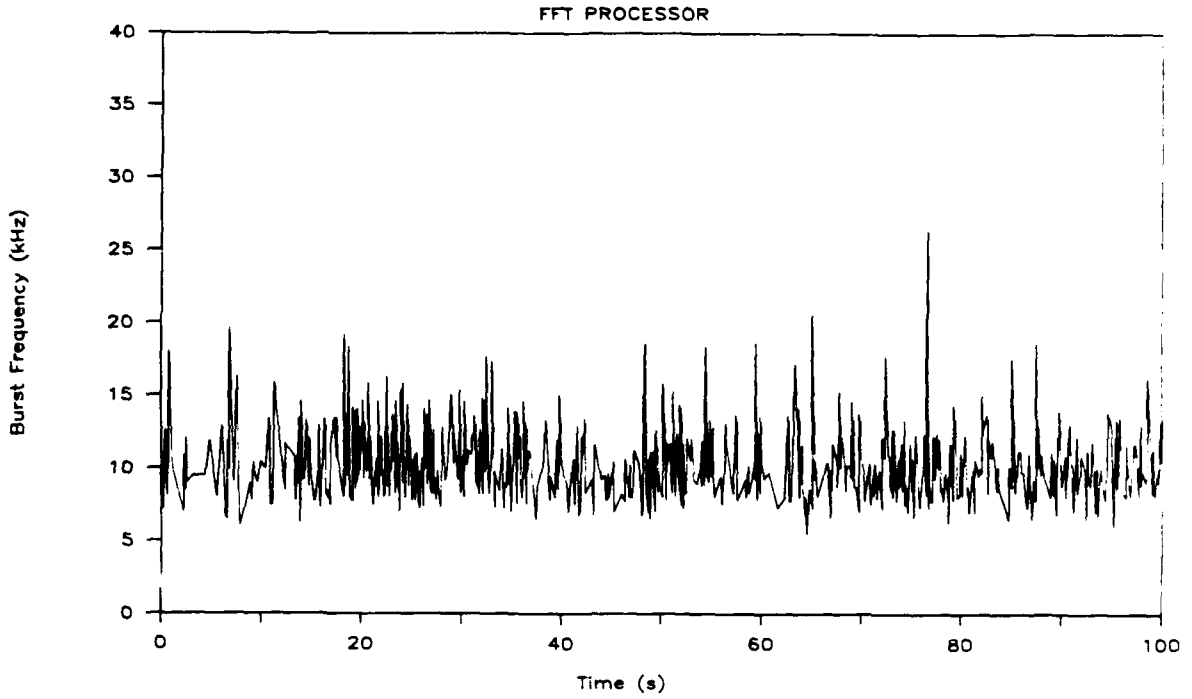

a. 10-second duration

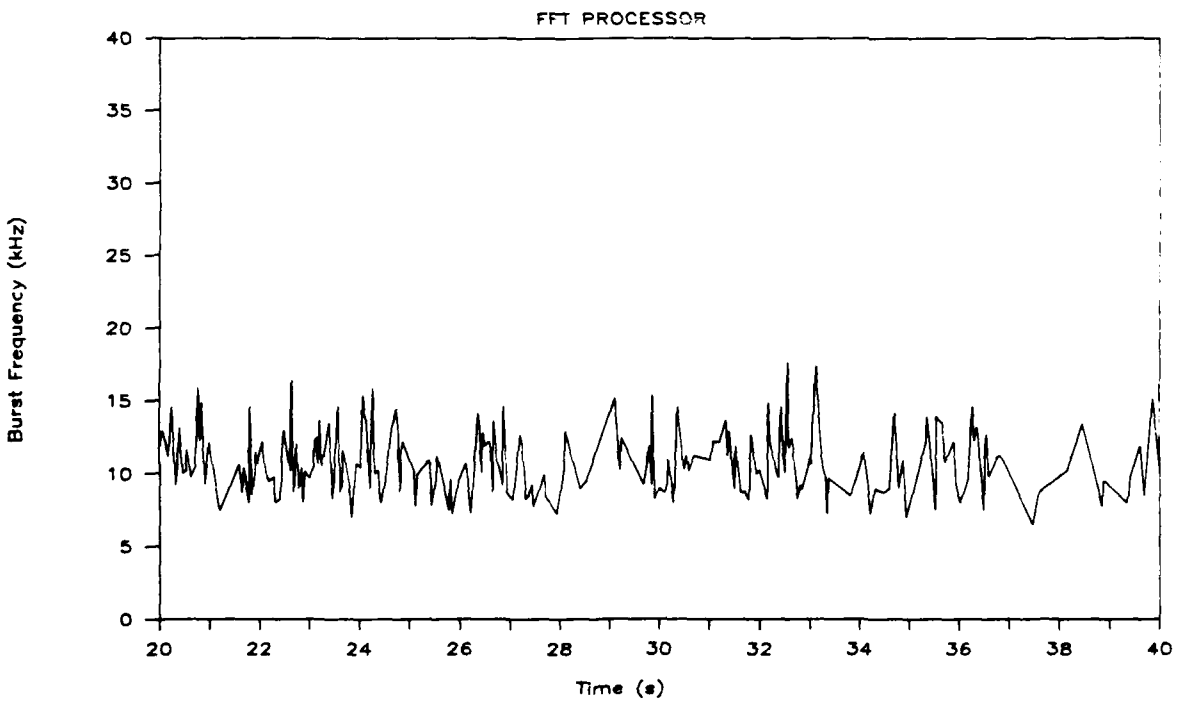

b. 20-second duration (expanded)

Figure 12. DLAV/FFT-Processor Measurements of the Longitudinal Velocity Component in a Turbulent Jet at x/D = 20 Along the Centerline

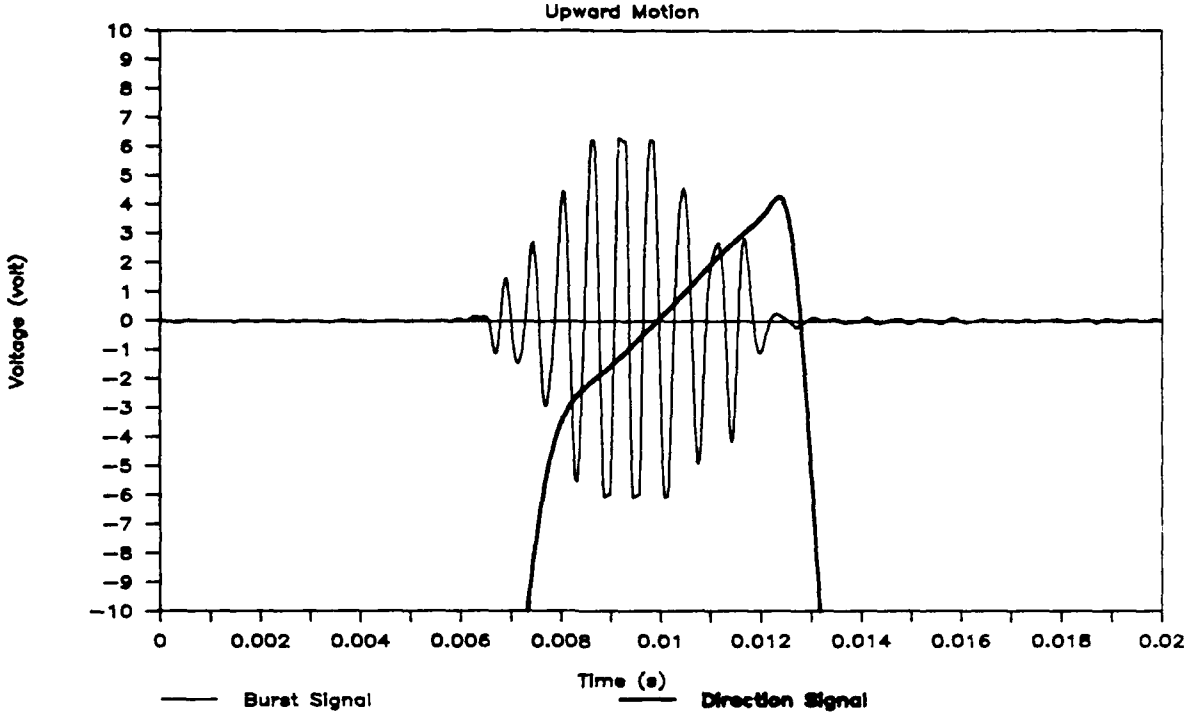

a. Upward Motion

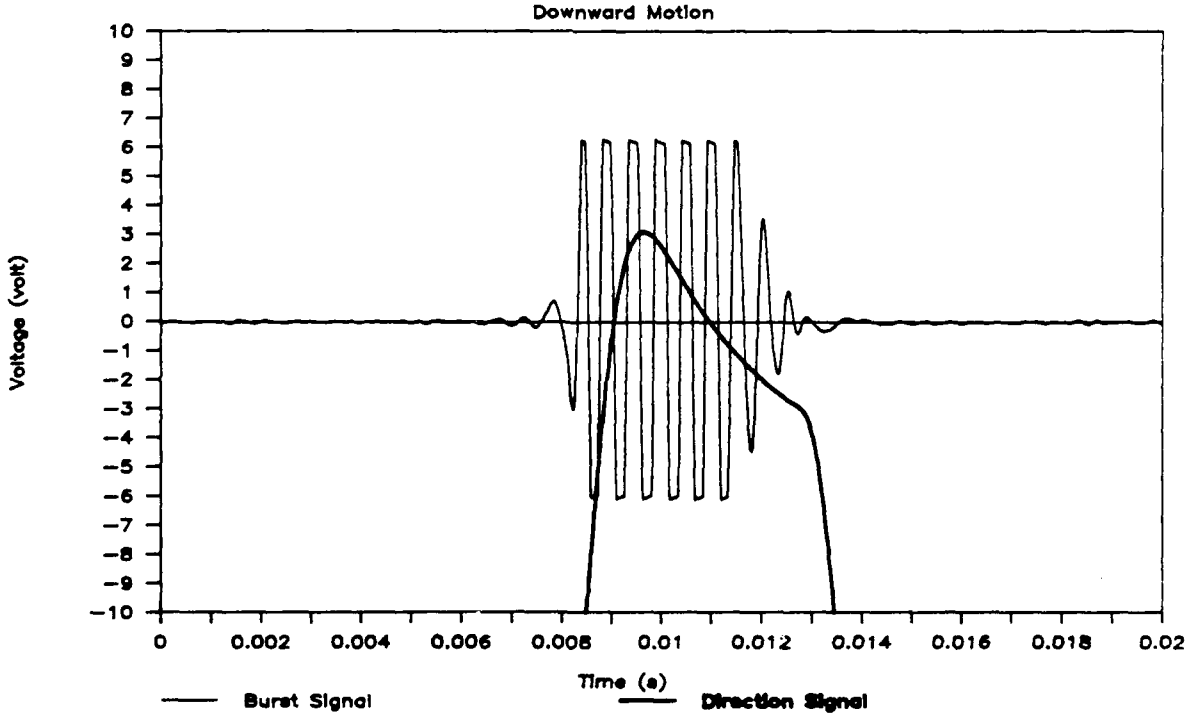

b. Downward Motion

Figure 13. Burst and Direction Signals in Response to Upward and Downward Motions of the Water Column

Note that the burst signals (forward scattered) have excellent SNR, whereas the directional signals (multiplied by 4) span only about one-tenth of the 10-V full range. Optimization may be achieved by fabricating smaller LE photodiodes for the intended application. The LE diode used in the DLDV/DS receiver has a dimension of 1 mm x 3 mm. Current technology exists to fabricate such a sensor with dimensions 2 to 3 times smaller than the one currently available to us. The advantage of using a small LE diode is at least twofold. First, it would increase the SNR of the direction and burst signals. Second, it would relax and simplify the requirements for the receiving optical systems, potentially leading to miniaturization of the optics and therefore the DLAV. During Phase II, effort will be made to acquire small-size LE diodes. For operation under a backscatter mode, LE diodes with significantly higher gain will be required. We will also consider the use of image intensifiers to improve the SNR.

The directional counter processor further processes the sum and difference of the signals illustrated in Figure 13 to calculate the burst frequency and the flow direction. The processed results are recorded via the data acquisition and analysis system. For a detailed description of the hardware and software installed in the processor, refer to Liu and Bondurant (1988). Typical processed results are illustrated in Figure 14. The abscissa and ordinate are, respectively, the time in milliseconds and the flow velocity in centimeters per second. The sampling rate was set at 50 Hz. The symbols represent the measured velocity data, and the solid curves are the best-fit representation of the oscillating flow using the following formula:

$$U = a \sin (b\ t + c) + d \qquad (1)$$

where a, b, c, d are the best-fit coefficients, t is the time in milliseconds, and U is the velocity in centimeters per second. For the present setup, the amplitude of oscillation is a = 6 cm/s and the period is 1/6 Hz. In the figure, the diamonds and triangles represent the uncorrected and corrected data, respectively. The data were corrected by checking the acceleration of the oscillating flow:

$$dU/dt = a\ b \cos (b\ t + c) \qquad (2)$$

For the condition with the water column oscillating at 1/6 Hz, The maximum velocity and acceleration are calculated at 6 cm/s and 6.3 cm/s^2, respectively. A data point with a wrong direction would result in a much larger value in the magnitude of the acceleration than the maximum value for the flow under consideration. For the one-dimensional flow, a simple sign change would correct for the error. For more complicated flows, a similar criterion may be applied during post analysis.

Figure 14a illustrates the uncorrected measurements together with the best-fit curve. There are six erroneous data points out of a total of 90 validated measurements, a 6.7%

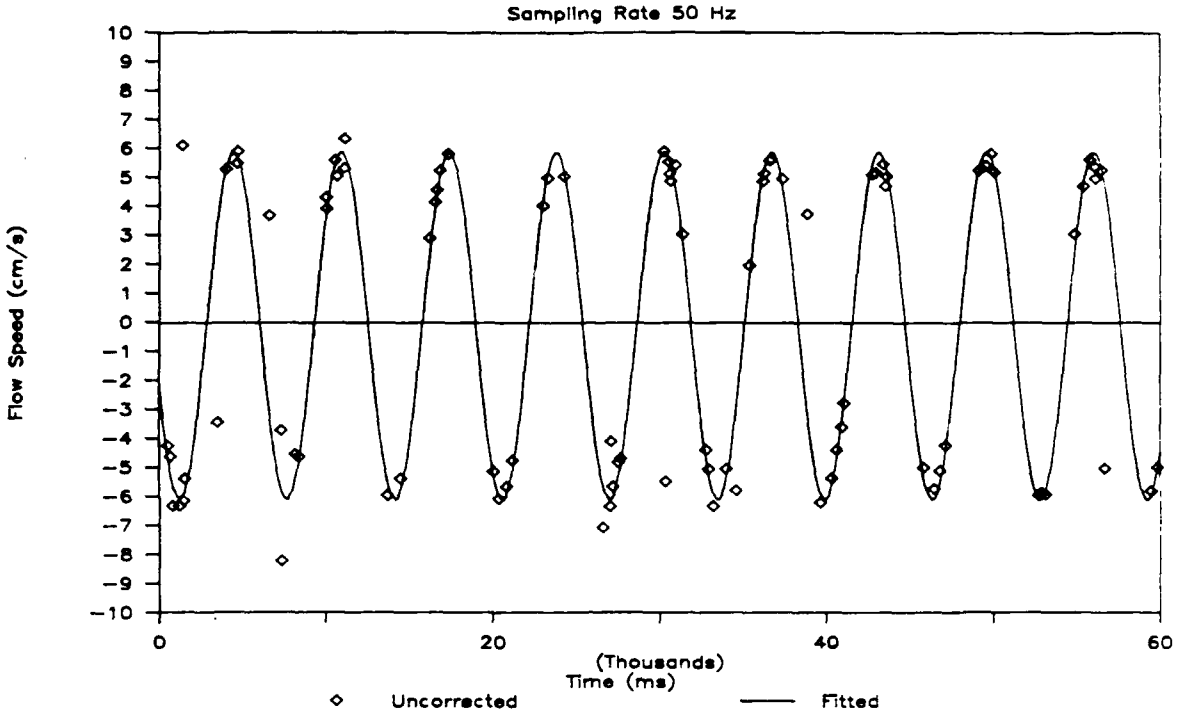

a. Uncorrected Results

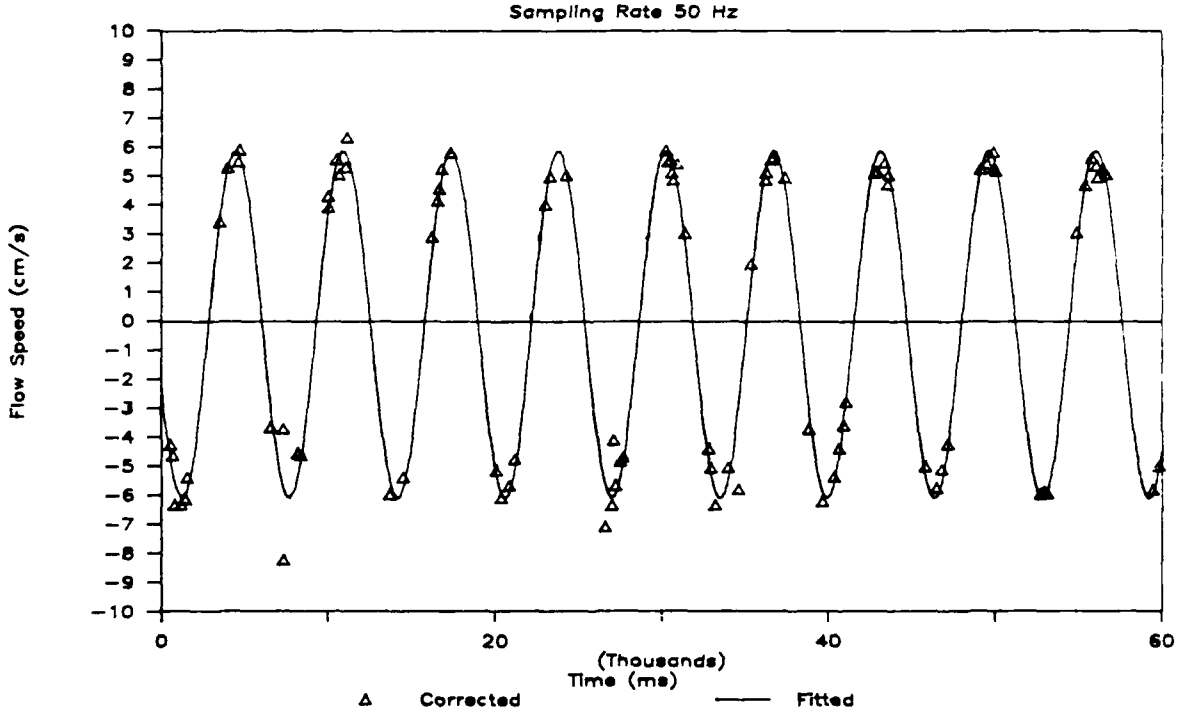

b. Corrected Results

Figure 14. DLAV Measurements of the Velocity of an Oscillating Water Column. The fringe spacing is ~35 μm; the DLDV/DS receiver and directional counter processor were used for removal of directional ambiguity.

erroneous occurrence. Due to the relatively large fringe spacing (35 μm), the errors are mainly due to the simultaneous presence of multiple particles in the focal volume, which confuses the directional sensing hardware and software. Under optimal conditions, the erroneous occurrence may reduce to less than 0.5%, as demonstrated in Figure 15, corresponding to the optimum configuration of the DLDV/DS measurements (Liu and Bondurant, 1988).

Applying the acceleration criterion described above, the corrected results are shown in Figure 14b. The corrected results agree well with the fitted curve, with few exceptions. As described by Liu and Bondurant (1988), the directional counter processor relies on the 5 (counts)/8 (counts) comparison convention to gauge the accuracy of the validation. Because the maximum number of zero crossings was limited to 10 for the 10-stripe diode array used for the DLAV model, we had to relax the accuracy by allowing a higher tolerance of inaccuracy. As a result, there was a relatively large error in the magnitude of the velocity measurements using the DLAV model. In contrast, the results measured with the DLDV/DS with a fringe spacing of 7.9 μm displayed excellent magnitude agreement with the fitted curves (see Figure 15).

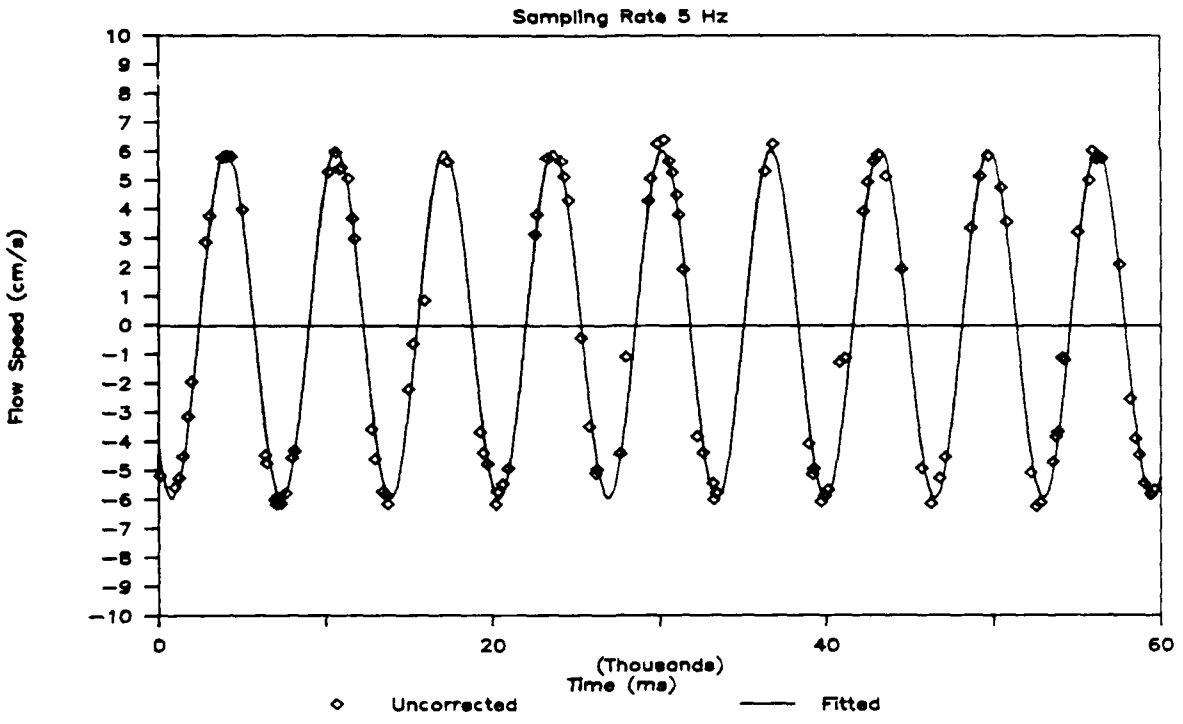

a. Sampling Rate of 5 Hz

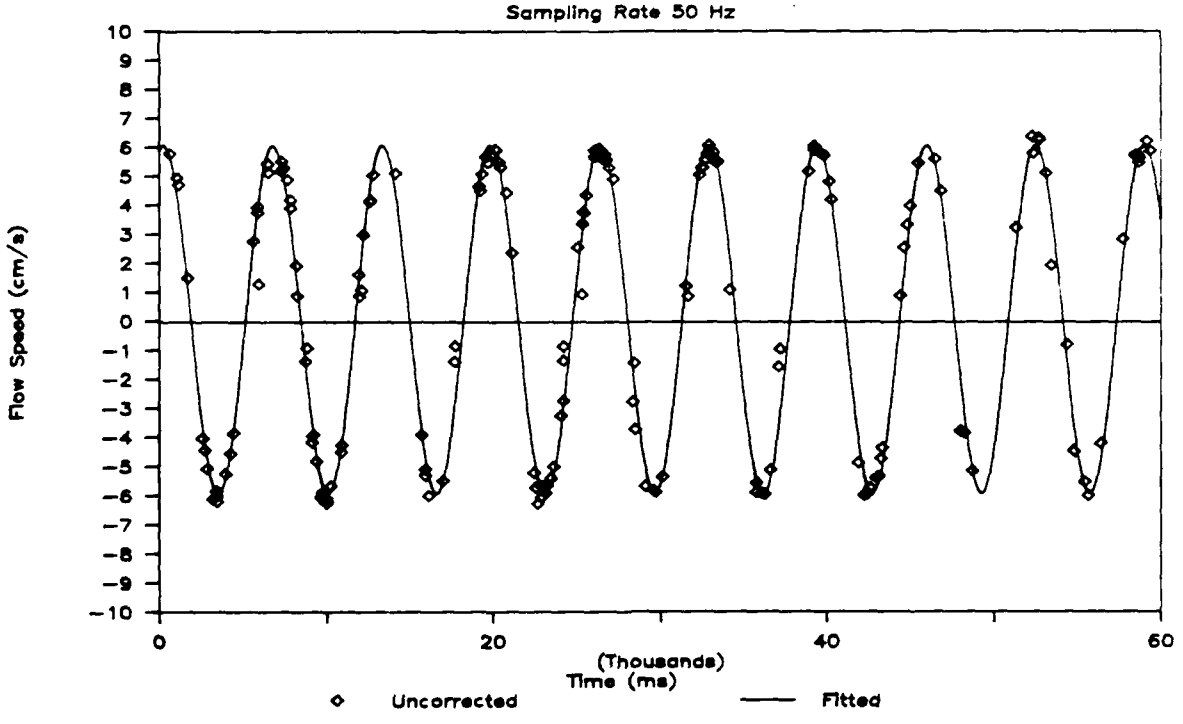

b. Sampling Rate of 50 Hz

Figure 15. Measurements of the Velocity of an Oscillating Water Column Using the DLDV/DS Under Optimum Conditions

6. SUMMARY AND RECOMMENDATIONS

In this section, we summarize the Phase I findings and assess the feasibility of the proposed development of a scanning diode laser velocimeter for field deployment in coastal and marine environments. Based on the results of a literature review and experiments conducted with a DLAV laboratory model in Phase I, we have demonstrated the feasibility of developing a scanning diode laser velocimeter. Recommendations for developing a scanning DLAV prototype during Phase II are also given in this section.

6.1 Summary

This Phase I investigation has shown that the originally proposed method failed due to current technological limitations in fabricating pulsed laser diodes. The original method proposed to replace the CW laser diode in the field-proven DLDV (Liu et al., 1985b, 1989) with a pulsed diode to achieve a gain in peak laser power of 2 to 3 orders of magnitude, which is necessary for backscatter operation of the scanning laser velocimeter. Our findings indicated that the current technology for solid-state laser diode fabrication is not capable of manufacturing pulsed laser diodes with an adequate coherence length for the emitting light and with a relatively long pulse width when operating at high power. The short coherence length (< 0.5 mm) would fail to form distinctive fringes at the sampling volume for relatively long-range projection, particularly when the difference in the optical paths of the two intersecting beams exceeds the coherence length. This would result in a poor SNR of the Doppler signals. On the other hand, the short pulse width (< 200 ns), would not accommodate the entire Doppler burst of low- to medium-speed flows. Although there are methods, such as generating "running" fringes to sweep across the slow-moving particles by shifting the frequency of one of the beams with a Bragg cell (see Section 4.2), we did not investigate these methods because there was no immediate solution to the problem of short coherence length, which is the most critical problem to be solved.

We subsequently resorted to high-power laser diode arrays in an attempt to develop a scanning diode laser array velocimeter (DLAV/S). Although the concept of a laser array velocimeter has been demonstrated by Dopheide et al. (1988), application of the LAV is limited to low-power arrays (< 200 mW), which display well-defined near-field fringes. The proposed development would require a diode array with power exceeding 1 W. For such high-power diode arrays, the amplitude of modulation of the near-field fringe pattern deteriorates with increasing laser power. In addition, there are many other relevant questions, such as signal processing, directional sensing, and image projection and signal detection, that must be dealt with before extending the LAV to a scanning and a backscatter configuration. To seek answers

to these questions, we designed, assembled, and tested a laboratory model of the DLAV using a low-power diode array (Sections 4.3 and 5.3). From the results of the laboratory experiments conducted with the DLAV model (Section 5.3), we assessed and demonstrated the feasibility of the proposed development of a scanning DLAV. The most important Phase I findings are as follows:

(1) Phase-locked diode arrays with CW laser power up to 5 W are available to date and would be a viable light source for a scanning DLAV for field deployment. A diode array is compact and may be driven by batteries--both of these features are desirable for deployment in remote sites. Diode arrays also have all the other advantages of a DLDV as described in Section 2.

(2) A laboratory model of the DLAV equipped with a 200-mW diode array as the light source was designed, assembled and tested during Phase I:
   - o A sampling volume of real fringes was formed by imaging the near-field pattern (Figure 6) of the array via a set of collimating lenses (Figure 7).
   - o It was configured to operate in an off-axis backscatter mode (Figure 7), as backscattered light collection is necessary for the scanning operation.
   - o The backscattered signals sensed slightly off axis have excellent signal-to-noise ratio (Figures 8 and 9).
   - o An FFT processor (Agrawal and Belting, 1988) was used successfully to measure the axial velocity components of a an air jet (Figures 10 through 12) under the backscatter mode.
   - o A directional counter processor (Liu and Bondurant, 1988) was also successfully used to measure the flow of an oscillating water column (Figures 13 and 14); the capability of direction sensing was provided by using a lateral-effect photodiode in conjunction with the processor.

(3) The feasibility of the proposed development has been demonstrated through a literature review of the state-of-the-art optronic components and a series of experiments using the DLAV laboratory model. A Phase II proposal is under preparation for the development of a prototype to be deployed in the field.

6.2 Recommendations

Several recommendations for the development of a prototype scanning DLAV for development in coastal and marine environments are given below:

(1) For the prototype DLAV, we recommend the use of a high-power diode array (1 to 5 W) as the light source. Such a power level is necessary for the backscatter configuration. Near-field real fringes will be generated by projecting the laser beam onto an amplitude grating. For measurements in the ocean body, we will consider the use of a green diode-pumped YAG laser (532 nm) as the light source. Currently, the maximum power is only about 5 mW; a prototype of a higher power version is under testing by Amoco Laser Company. The combination of extremely low attenuation of sea water (the 50% attenuation length is about 30 times larger than that at 800 nm) and high quantum efficiency of the photomultiplier at this wavelength may be more than compensating for the low laser power, especially when higher power units will be available in the near future. In addition, the large coherence length and small beam divergence of the YAG laser (75 m) is less restrictive in the scanning range.

(2) For high-power diode arrays, the near-field light pattern becomes a top-hat configuration without the large-amplitude modulation of those of their low-power counterparts. To recreate the near-field pattern with a large-amplitude modulation, we will have to project the laser light onto an amplitude grating and project the recreated near-field to the sampling volume. In that process, only half of the laser power would pass through the grating. For the diode-pumped YAG, with a coherence length greater than 5 m, a phase grating may be used to generate the real fringes, and only a small percentage of the laser power will be lost.

(3) For a grating with a fixed spacing, the fringe spacing at the sampling increases with increasing scanning range. To avoid a high probability of the simultaneous presence of multiple particles in the sampling volume, which would cause a high rate of dropout, it is necessary to use a relatively small fringe spacing. For example, the maximum allowable fringe spacing should be about 15 μm, depending on the number density of the natural particles in the field. The combination of the specifications of the optics for projection/receiving and the maximum fringe spacing would dictate the maximum scanning range for the proposed system. One of the main tasks in Phase II

will be to design and optimize the scanning optics to achieve a scanning range of 2 to 3 m. For example, we may use a reflector instead of a lens for projection/receiving, as diffraction-limited reflectors are much easier to fabricate than lenses, especially large-diameter lenses.

(4) We will consider developing a grating with a variable spacing that is tied to the scanning distance. The idea is to maintain a constant fringe spacing independent of the scanning distance. Such a development, if successful, would considerably simplify the hardware and software for data processing. For example, Figure 16 is a schematic of a scanning DLAV with a constant fringe spacing. In the design, a voice coil will be used to move the collimating optics for scanning the sampling volume. A key element is a photo-elastic modulator. A feedback circuitry will be developed to vary the frequency of the piezo transducer driver, which controls the spacing of the grating. In the figure, the laser light is polarized to facilitate backscatter collection using the same set of scanning optics.

(5) For directional sensing in backscatter, we will consider a geometry invented and patented by Agrawal (Agrawal and McCullough, 1981; McCullough and Agrawal, 1988). In this concept, a single laser beam is transmitted to the sample volume. The beam waist has no structure; it is simply a focussed Gaussian beam. Instead, structure is built into the detector. An array of sensors is placed at the plane containing the backscattered image of the sample volume. The elements of the array are electrically connected in such a manner that alternate elements produce a positive photocurrent, and the other alternate set, a negative. As the image of a scatterer travels across the detector array, the alternating detector elements produce an alternating current, of frequency equal to the ratio of the image velocity to array spacing. For direction sensing, the period in the response of the array is changed to four elements, in contrast to two above. This makes two periodic arrays, offset by a quarter period, so that the two signals are in quadrature. Using these two signals as the real and imaginary parts of a complex signal, the sign of frequency is obtained.

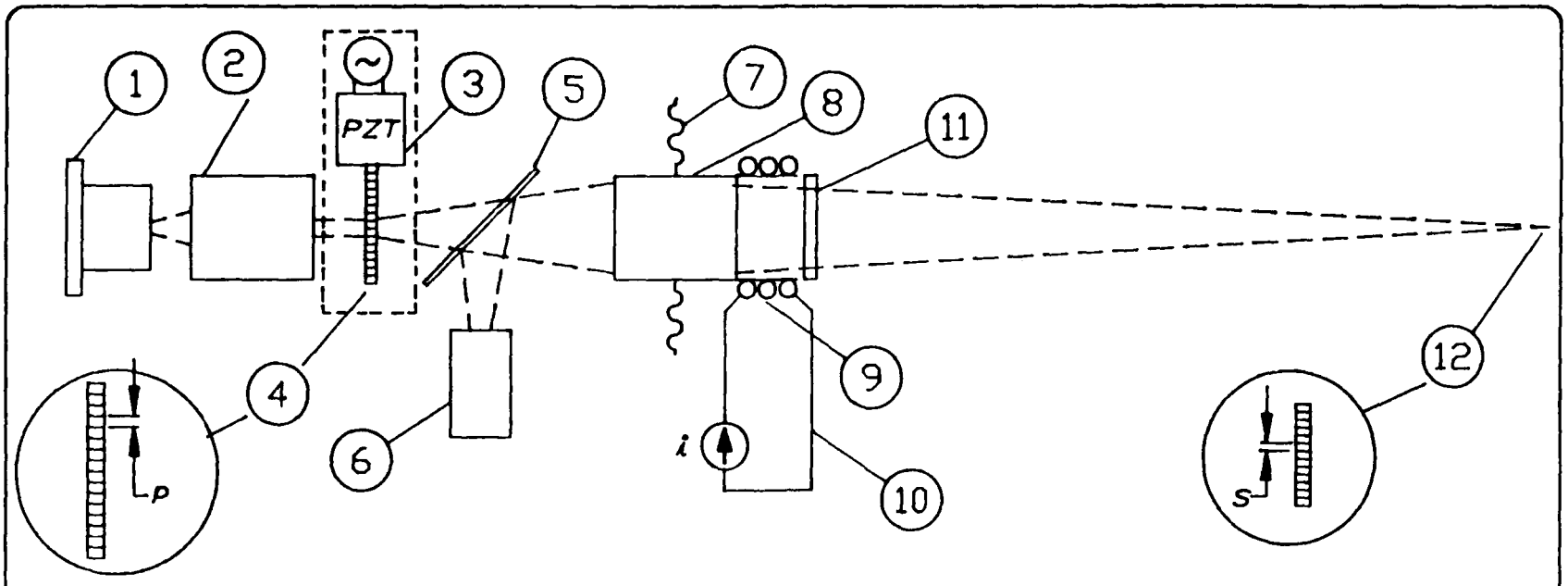

PARTS LIST	
ITEM	DESCRIPTION
1	HIGH–POWER LASER DIODE ARRAY (2~5W)
2	SHORT FOCAL–LENGTH COLLUMATING LENSES
3	PHOTO–ELASTIC MODULATOR WITH FREQUENCY fg
4	VARIABLE GRATING p
5	QUARTER–WAVE THIN BEAM SPLITTER PLATE
6	PHOTOSENSOR
7	FLEXIBLE MOUNT
8	OSCILLATING COLLUMATING LENSES FOR
	SCANNING THE FOCAL VOLUME
9	VOICE COIL
10	CURRENT LOOP FOR DRIVING VOICE COIL
11	QUARTER WAVE PLATE
12	IMAGE OF (4) WITH GRATING SPACING "S"

DESIGN CRITERIA:

POSITION OF $X = f_s(i)$

SPACING $p = \frac{1}{[fg\,K(i)]}$

SPACING IS INDEPENDANT OF PROJECTION DISTANCE

REVISIONS

5/10/89

DR

PETER LIU

NONE

FLOW INDUSTRIES, INC.
21414 68th AVE. SOUTH
KENT, WASHINGTON 98032

FIGURE 16

GD23–002

Figure 16. Schematic of a Scanning DLAV for Phase II R&D

REFERENCES

Agrawal, Y. C. (1984) "A CCD Chip-Z FFT Doppler Signal Processor for Laser Velocimetry," *J. Phys. E (Sci. Instr.)*, Vol. 17, pp. 458-461.

Agrawal, Y. C., and Belting, C. J. (1988) "Laser Velocimetry for Benthic Sediment Transport," *Deep Sea Res.*, Vol. 35, pp. 1047-67.

Agrawal, Y. C., and McCullough, J. R. (1981) "Directional, Pedestal-Free Laser Doppler Velocimetry without Frequency Biasing: Part I," *Applied Optics*, Vol. 20, pp. 1553-1556.

Agrawal, Y. C., Aubrey, D. G., and Dias, F. (1988) "Field Observations of the Coastal Bottom Boundary Layer Under Surface Gravity Waves," presented at the 4th Int. Conf. on App. to Laser Anemometry to Fluid Mechanics, Lisbon, Portugal, July 11-14.

Chumbley, P. E. (1989) "Microlasers Offer New Reliability for R&D," *Research and Development*, June, pp. 72-76.

Dopheide, D., Faber, M., Taux, G., and Reim, G. (1988) "The Application of Phase-Coupled Diode Arrays for LDA and for a New Technique: The Laser Array Velocimeter (LAV)," presented at the 4th Int. Conf. on App. of Laser Anemometry to Fluid Mechanics, Lisbon, Portugal, July 11-14.

Durst, F., Melling, A., and Whitelaw, J. H. (1976) *Principles and Practices of Laser Doppler Anemometry*, Academic Press, New York, 405 pp.

Durst, F., Howe, B., and Richter, G. (1980) "LDA-System Design for Long-Range Wind-Velocity Measurements," *Proceedings of the Symposium on Long Range and Short Range Optical Velocity Measurements*, September 15-19.

Kuntz, D. (1984) "Specifying Diode Laser Diode Optics," *Laser Focus/Electro-Optics*, March, pp. 44-55.

Liu, H.-T. (1986) "Development of a Diode Laser Velocimeter with Directional Sensing Capabilities," Flow Technical Report No. 366, Flow Research, Inc., March.

Liu, H.-T., and Bondurant, P. D. (1988) "A Field-Worthy Diode Laser Doppler Velocimeter with Directional Sensing Capability: Prototype Development," Flow Research Report No. 450 (prepared for U.S. Department of Energy under Contract No. DE-AC03-85ER80244).

Liu, H.-T., and Lin, J.-T. (1987) "Measurements of Wave-Variance and Velocity Spectra in Breaking Waves," *Experiments in Fluids*, Vol. 5, pp. 201-212.

Liu, H.-T., Kollé, J. J., and McPhee, M. G. (1985a) "Development of a Diode Laser Doppler Velocimeter for Measurements in the Oceanic Boundary Layer Under Ice" (Abstract only), *EOS*, Vol. 66, No. 18, April.

Liu, H.-T., Kollé, J. J., and Bondurant, P. D. (1985b) "A High-Resolution Cluster of Oceanographic Instruments for Boundary Layer Measurements Under Ice," Flow Research Report No. 352, November.

Liu, H.-T., Kollé, J. J., and Bondurant, P. D. (1989) "Development of Field-Worthy Diode Laser Doppler Velocimeters," to appear in *Proceedings of Oceans '89*, September 18-21, Seattle, WA.

McCullough, J., and Agrawal, Y. C. (1988) "Method for Measuring Particle Velocity Using Differential Photodiode Arrays," U.S. Patent No. 4,725,136 (assigned to U.S. Navy).

McPhee, M. G. (1985) "Comparison of Diode-Laser-Doppler Velocimeter and Medium Resolution Turbulence Cluster Measurements in MIZEX 84," Technical Report 85-1, McPhee Research Company, Yakima, Washington.

Schedvin, J. C., and Liu, H.-T. (1984) "The Development of a Diode Laser Doppler Velocimeter for Boundary Layer Measurements Under Ice: A Feasibility Investigation," Flow Technical Report No. 290.

Sharpe, P. R. (1979) "An On-Line Data Reduction System for Photon Correlation Laser Anemometry," *Physica Scripta*, Vol. 19, pp. 411-416.

Spectra Diode Labs (1988) "Laser Diode Operator's Manual & Technical Notes," Spectra Diode Labs, DCL 001 EB, November.

APPENDIX

A BRIEF DESCRIPTION OF THE FIRST-GENERATION DLDV

In this Appendix, we describe briefly the first-generation DLDV developed at FLOW. Detailed information is given by Schedvin and Liu (1984) and Liu et al. (1985b). Special characteristics of the laser diodes that are used as the light source of a diode laser are noted.

A.1 Diode Laser Doppler Velocimeter

The DLDV was developed originally for use in the ocean boundary layer under ice floes in the Arctic Ocean. The DLDV replaces the gas laser (He-Ne laser) used in a laser Doppler velocimeter (LDV) with a diode laser (DL). Figure A-1 shows a schematic of the DLDV, which includes transmitting and receiving modules, operating in the forward-scatter mode. The transmitting module consists of a single-mode solid-state laser diode (LD), a low-power DC power supply, and a set of optics for collimation, beam splitting, and focusing. The DL is installed in a sealed housing (4 cm in diameter x 15 cm long) for underwater applications. The receiving module consists of a photodiode, a low-power DC power supply, an amplifier

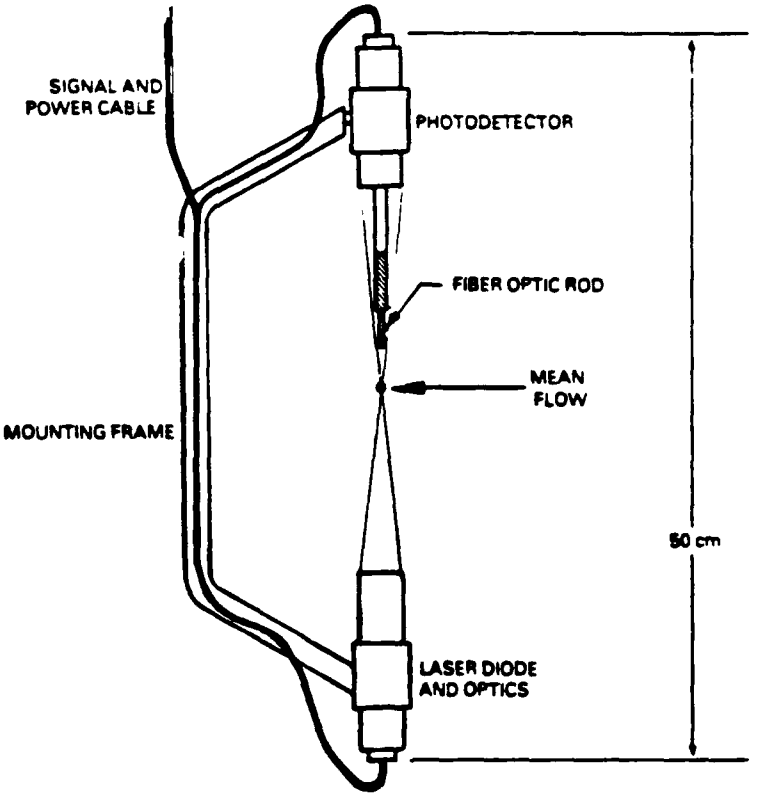

Figure A-1. Prototype DLDV Design for Field Test

circuitry, and a fiber optic rod for collecting the scattering light at the focal volume. These components are housed separately in a sealed cylinder (4 cm in diameter x 10 cm long). From the above description, the compactness and the ruggedness of the DLDV are apparent.

Figures A-2 and A-3 show two Doppler burst signals (with the low-frequency pedestal removed) measured in a pipe flow (filled with tap water passing through a 10-micron filter) with the DLDV and an LDV using a 5 mW He-Ne laser as the light source. While the Doppler burst with the He-Ne laser was higher on the average than that obtained with the laser diodes, the noise level was lower for the laser diodes. Thus, the signal-to-noise ratio, considered as the ratio of the rms voltage in a Doppler burst to the rms background noise in the photodetector output, was found to be essentially equivalent. In water, the extinction coefficient is higher for the laser diode light (780 to 850 nm) than for the He-Ne light (632 nm). This is roughly compensated for by the better response of the silicon photodiode to the former than to the latter.

The DLDV has been successfully tested in the laboratory using water droplets (in air) or powdered milk (in water) as the tracers and in the Arctic Ocean using natural tracers (Schedvin and Liu, 1984). In the forward-scatter mode, test results (e.g., Figures A-2 and A-3) show that the DLDV works at least as well as an established LDV using a He-Ne or an argon-ion laser as the light source. During July 1984, two prototype DLDVs were deployed for measuring ocean current and turbulence under an ice floe in the marginal ice zone (MIZ) in the Fram Straits of the Greenland Sea (Schedvin and Liu, 1984; McPhee, 1985). Three high-resolution clusters (with a spatial resolution of about 1 to 2 cm), including three-component DLDVs, temperature and conductivity probes for measuring momentum, heat and mass fluxes were also deployed in the Arctic Ocean during the Arctic Internal Wave EXperiment held in March 1985 (designated as AIWEX 85). The Office of Naval Research (ONR) is the sponsor of both experiments. For AIWEX 85, the velocity-temperature-conductivity (V-T-C) clusters were controlled by a microprocessor, which was used for data acquisition from calibration of the sensors, setting up the experimental configuration, and processing and manipulation of the data to recording. A set of software will be developed for data analysis.

A.2 Important Characteristics of Laser Diodes

There are a large number of laser diodes available commercially, but only a few have characteristics that are suitable for use as the light source of a laser for LDV applications. For a more detailed description of the laser diodes, refer to the manual by Spectra Diode Labs (1988). The laser diode characteristics that are of the greatest importance include the wavelength of the emitted laser light and the laser coherence length. Other important

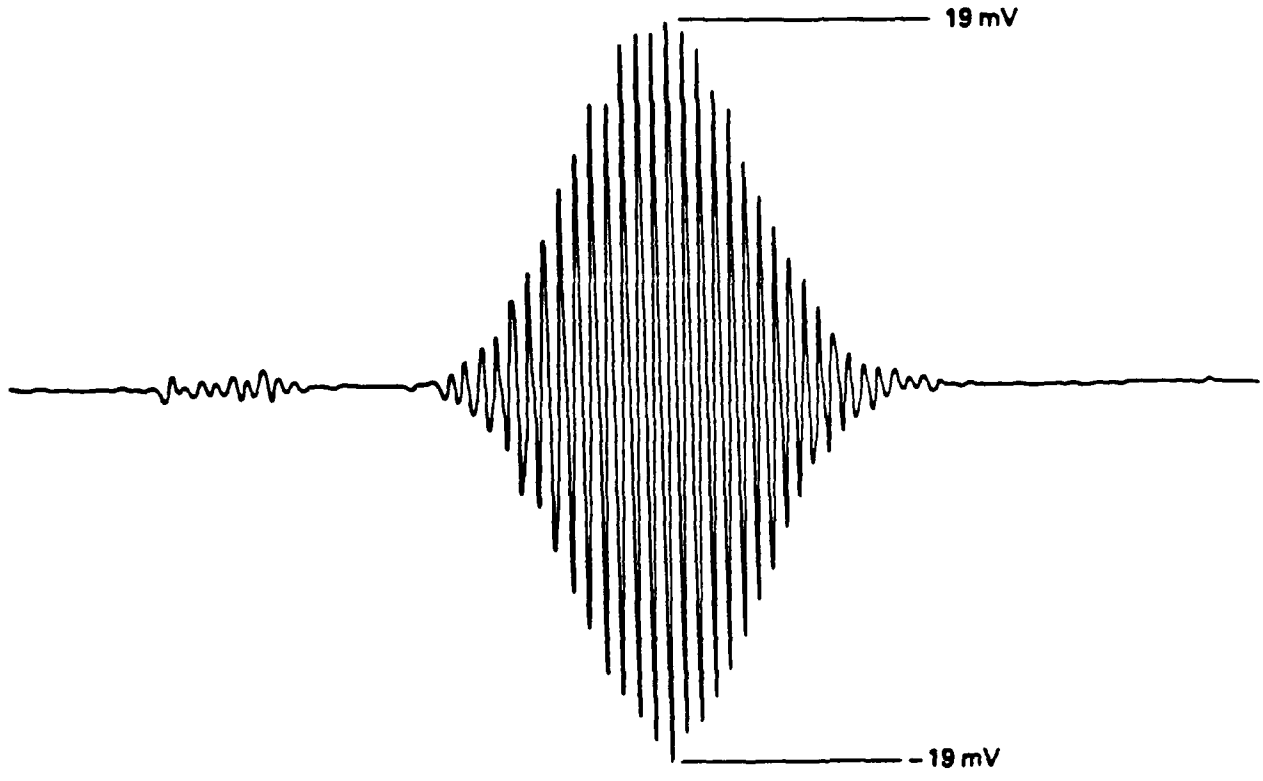

Figure A-2. Typical Doppler Burst with SCW-21 Laser Diode and Fiber Optics Rod Pickup. Filter band-pass - 40 to 200 kHz; background noise - 0.09 mV rms; Doppler frequency - 85.9 kHz = 51.0 cm/s.

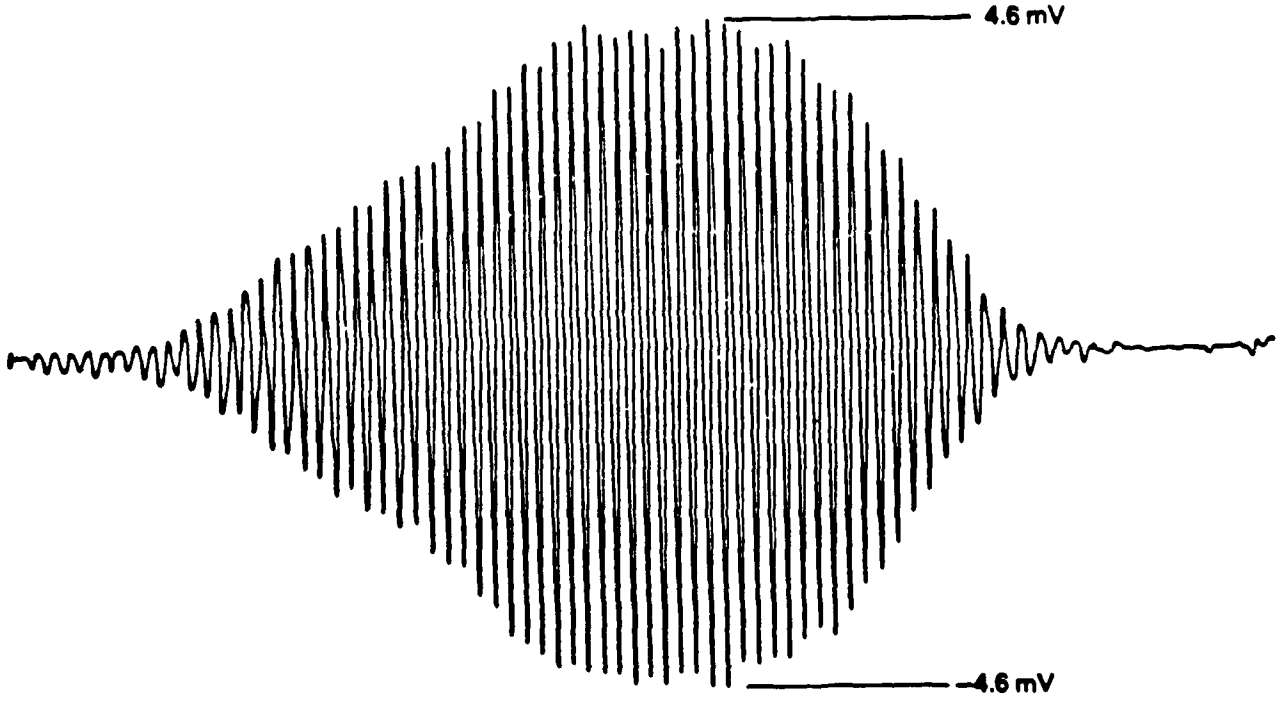

Figure A-3. Large Doppler Burst with He-Ne Laser Using Lenses to Focus Scattered Light on Photodiode. Filter band-pass - 25 to 70 kHz; background noise - 0.24 mV rms; Doppler frequency - 57.8 kHz = 26.4 cm/s.

characteristics are the laser diode output power and the divergence of the laser beam. In the following, we briefly describe a few of these characteristics. As a coherent light source of the LDV, the laser diode (single-element, index guided) has several special features that are different from those of the He-Ne laser:

(1) The collimated light beam of a laser diode is elliptical in shape and so is the focal volume of the DLDV. Depending on the orientation of the diode, one may have the fringe pattern aligned in the direction of the major or minor axis of the ellipse; there are about 3 times more fringes in the former orientation than in the latter. If desired, special optics are available to shape and truncate the beam into a circular pattern (Kuntz, 1984).

(2) The laser light has a wavelength between 670 and 850 nm. The laser light with wavelengths exceeding 780 nm is not visible unless it is viewed with a fluorescent screen. In water, the absorption of the deep red light is stronger than that of the He-Ne light (632 nm). This is somewhat compensated for by the higher response and efficiency of the photodiode to the deep red light than to the red light.

(3) The coherence length of the diode laser, defined as $\lambda^2/\Delta\lambda$ where λ is the peak wavelength of the emission spectrum and $\Delta\lambda$ is the spectral bandwidth of the laser light. According to Sharp Electronics, the coherence length of the Model LT024M is about 10 m, which is somewhat shorter than that of a He-Ne laser.